

## **Distribution Agreement**

In presenting this thesis as a partial fulfillment of the requirements for a degree from Emory University, I hereby grant to Emory University and its agents the non-exclusive license to archive, make accessible, and display my thesis in whole or in part in all forms of media, now or hereafter known, including display on the world wide web. I understand that I may select some access restrictions as part of the online submission of this thesis. I retain all ownership rights to the copyright of the thesis. I also retain the right to use in future works (such as articles or books) all or part of this thesis.

Signature:

---

Jared Henry Gans

---

April 15, 2010

Studies of Mechanisms of Lipid Binding by the Adaptor Protein Complex AP-3 using Single and Bulk Molecule Fluorescence *in vitro* Assays.

By

Jared Henry Gans

Adviser

Ivan Rasnik, Ph.D.

Program in Neurosciences and Behavioral Biology

---

Ivan Rasnik, Ph.D.  
Adviser

---

Victor Faundez, Ph.D.  
Committee Member

---

Paul Lennard, Ph.D.  
Committee Member

---

Ronald Calabrese, Ph.D.  
Committee Member

---

April 15, 2010

Studies of Mechanisms of Lipid Binding by the Adaptor Protein Complex AP-3 using Single and  
Bulk Molecule Fluorescence *in vitro* Assays.

By

Jared Henry Gans

Adviser

Ivan Rasnik, Ph.D.

An abstract of  
A thesis submitted to the Faculty of Emory College of Arts and Sciences  
of Emory University in partial fulfillment  
of the requirements of the degree of  
Bachelor of Sciences with Honors

Program in Neuroscience and Behavioral Biology

2010

## Abstract

Studies of Mechanisms of Lipid Binding by the Adaptor Protein Complex AP-3 using Single and Bulk Molecule Fluorescence *in vitro* Assays.

By Jared Henry Gans

The mechanism behind guidance of intracellular vesicles is an active field of study in Cell Biology. Protein-lipid binding serves an important method in this guidance. Specifically, adaptor proteins complexes (APs) such as AP-3 and the phospholipids they bind and concentrate in vesicles have been shown to be important in the specificity of this mechanism. However, the dynamics of vesicle budding and the role of the different components, in particular lipids, on this process have not been directly studied. Reported here is the study of these protein-lipid interactions through *in vitro* model systems. The interactions of streptavidin with biotinylated phosphoethanolamine and of AP-3 with fluorescently labeled phosphatidylinositol 4-phosphate were tracked at the single molecule and bulk levels within solid supported lipid bilayers of phosphocholine on quartz slides. Their interactions with their respective proteins were characterized by changes in their diffusion coefficients as measured by Single Particle Tracking and Fluorescence Correlation Spectroscopy. Additionally, an antibody immobilization assay for protein binding imaged by Total Internal Reflection Fluorescence Microscopy was developed. While no change in phosphatidylinositol diffusion was observed in the presence of AP-3 for any of the systems, a distinct and unexpected drop in diffusion was found for the biotin-streptavidin system. This effect proved dependent on solution viscosity and illustrates a novel drag force on the bound protein slowing down lipid diffusion within the bilayer.

Studies of Mechanisms of Lipid Binding by the Adaptor Protein Complex AP-3 using Single and  
Bulk Molecule Fluorescence *in vitro* Assays.

By

Jared Henry Gans

Adviser

Ivan Rasnik, Ph.D.

A thesis submitted to the Faculty of Emory College of Arts and Sciences  
of Emory University in partial fulfillment  
of the requirements of the degree of  
Bachelor of Sciences with Honors

Program in Neuroscience and Behavioral Biology

2010

## Acknowledgements

I would like to thank Dr. Ivan Rasnik for being the Primary Investigator of this project and showing the open-mindedness to inspire and oversee a NBB Thesis. I would also like to thank Dr. Victor Faundez for additionally providing guidance and resources on this project. I would like to thank Julie Coats, Dr. Yuyun Kent Lin, and the members of the Faundez Lab for providing guidance with techniques. I would like to thank Ben Kesler for providing programming assistance.

Additionally, I would like to thank the members of my committee for being patient and enthusiastic in meeting on the project. This includes Dr. Ivan Rasnik and Dr. Victor Faundez as well as Dr. Paul Lennard and Dr. Ronald Calabrese. A special thanks is necessary to Alan Weinstein and Nadia Brown for helping put together honors committee meetings.

I would finally like to thank my family and friends without whose support this project would never have been undertaken in the first place. This is especially true for my parents Howard and Hillary, my brother Logan, and my grandparents Stuart and Frann Raider.

Funding for this project was provided by grants from the National Science Foundation and National Institutes of Health.

## Table of Contents

I.	Introduction .....	1
	a. Model Membranes.....	1
	b. Single Molecule and Bulk Studies of Lipid Supports .....	3
	c. Adapter Complexes .....	7
II.	Materials and Methods.....	10
	a. Lipid Materials .....	10
	b. AP-3 Purification .....	10
	c. Slides .....	11
	d. SUV Formation .....	12
	e. SLB Formation .....	12
	f. Biotinylated SLBs .....	13
	g. TIRFM .....	13
	h. FCS .....	14
	i. Viscosity Tests of Biotinylated SLBs.....	14
	j. AP-3 Immobilization.....	15
	k. Data Analysis.....	16
III.	Results .....	16
	a. TIRFM of Biotinylated Bilayers .....	16
	b. FCS of Biotinylated Bilayers and Effects of Viscosity .....	17
	c. TIRFM of PIP systems with and without AP-3 .....	17
	d. FCS of PI4P, RhPE .....	18
	e. Nonspecific Binding Check for Antibody Immobilization .....	18
	f. AP-3 Binding with Antibodies .....	18
IV.	Discussion.....	19
	a. TIRFM and FCS of Biotinylated SLBs .....	19
	b. TIRFM of Labeled Phosphoinositides PI4P and PI(4,5)P2.....	20
	c. TIRFM of AP-3 and Labeled PI4P .....	21
	d. AP-3 Immobilization .....	21
V.	Conclusions.....	22
VI.	References.....	24
VII.	Figures and Tables.....	29

## List of Tables and Figures

I.	Figure 1 .....	29
II.	Figure 2 .....	30
III.	Figure 3 .....	31
IV.	Figure 4 .....	32
V.	Figure 5 .....	33
VI.	Figure 6 .....	34
VII.	Figure 7 .....	35
VIII.	Figure 8 .....	36
IX.	Figure 9 .....	37
X.	Figure 10 .....	38
XI.	Figure 11 .....	39
XII.	Figure 12 .....	40
XIII.	Figure 13 .....	41
XIV.	Figure 14.....	42
XV.	Figure 15 .....	43
XVI.	Figure 16 .....	44
XVII.	Figure 17 .....	45
XVIII.	Table 1.....	46
XIX.	Figure 18.....	47

## **Introduction**

Intracellular vesicular guidance is an important function of cell physiology in living cells. Molecules produced in an organelle in one part of a cell need to be successfully carried to other cell locations. Moreover, many components are used multiple times and thus retrieval of transport machinery back to the donor compartment by vesicles is necessary in order to maintain homeostatic balance and function of normal cellular machinery. Guidance for vesicles carrying particular proteins or chemicals additionally allows for their asymmetrical distribution throughout larger cells, such as neurons. In the case of neurons, this allows for localization of these components necessary for proper synaptic transmission and maintenance. In order for this guidance to occur, proteins must show some sort of specificity to lipids within the cellular membrane (Faundez et al., 2007; Paolo & Camilli, 2006).

## **Model Membranes**

The dynamics of the lipids which make up cellular membranes in general remain a mystery. The Fluid-Mosaic Model presents a scenario where proteins and lipids move freely within a membrane in the form of a bilayer (Singer & Nicolson, 1972). However, biological membranes are made up of a variety of lipids and proteins each with their own specific dynamics. For instance, individual lipid varieties have their own specific transition temperature ( $T_m$ ) at which lipid mixtures switch from a solid “gel” phase to a liquid phase which can aggregate into vesicles. Changes in temperature can thus affect how lipids behave in the membrane and differences in  $T_m$  can affect how different lipids mix together (Boggs, 1987; Nagle, 1980). Simultaneously, proteins and cholesterol within membranes can cause their own changes in membrane fluidity and local lipid concentrations (Kleemann & McConnell, 1976;

Veatch & Keller, 2002). This relationship between varied lipids, proteins, and cholesterol within the membrane presents a far more complicated scenario than the Fluid-Mosaic Model initially presents.

The study of the effects of asymmetric distributions of lipids within the membrane and the way in which these microdomains are produced has been an active area for research of this scenario in recent years. Diffusion rates for these constituent lipids fluctuate and thus different constituents are able to create different environments within biological membranes (Tocanne et al., 1994). These “lipid rafts” can serve as a source of secondary messaging and organization within the cell by coordinating directly with proteins (Edidin, 2003). It is thought that this messaging system is involved in everything from disease pathogenesis to intracellular signaling (Edidin, 1997; Simons & Ehehalt, 2002). The prospect of studying the formation of these lipid rafts under controlled conditions therefore presents a possibly productive avenue for research.

The study of these lipid systems *in vitro* as model membranes presents several advantages over the study of living cells. Molecular studies in living cells typically produce an aggregate signal for the entire cell as a result. Additionally, living cells contain cytoskeletal elements, integral membrane proteins, cholesterol, and other chemical compounds which may stabilize lipid microdomains themselves. Thus, a single molecule study of lipid movements within living cells represents a number of challenges for ascertaining the nature of membrane dynamics (Sako & Yanagida, 2003). A model membrane system’s composition, on the other hand, can be more easily manipulated and tracked by more sensitive means.

Model membrane systems currently have a vast array of avenues for simulation of the biological membrane. The formation artificial vesicles through sonication or extrusion of

various lipid mixtures have been sources for the study of Small Unilamellar Vesicle (SUV) systems for some time (Barenholz et al., 1977; Olson et al., 1979). The use of supported lipid bilayers (SLBs) made from fusion of these vesicles provides a scheme for the study of planar membrane dynamics. Past work in analysis of the immune system components' relationship with the membrane showed that SLBs provided a superior environment compared to simple vesicular systems when studying the interactions of individual molecules with the membrane (McConnell et al., 1986). The fusion of SUVs when in the proper density and exposed to a polar solid surface (glass and quartz) has been well characterized at the single molecule level through tracking of a small concentration of fluorescently tagged lipids in the original SUVs (Johnson et al., 2002). However, studies of the diffusion coefficients among SLBs on solid supports compared to those with SUVs have shown a decrease in molecular mobility within the model membrane, especially with the introduction of integral membrane proteins (Tocanne, et al., 1994). An attempt to solve this issue has been the use of polymer-supported lipid bilayers over direct deposition onto the solid surface, but an inability of these efforts to produce a continuous stable membrane consistently has proven an obstacle (Wagner & Tamm, 2000). Additionally, these polymers may have their own confounding effects on membrane domain formation (Zhang & Granick, 2005). Therefore, solid-supported lipid bilayers remain the optimal way to study free protein interactions with a continuous planar lipid membrane at high levels of specificity.

### **Single Molecule and Bulk Studies of Lipid Supports**

The study of lipid dynamics within the SLB has remained problematic. As mentioned earlier, lipid diffusion in different model membrane systems varies (Tocanne, et al., 1994). In general, lipids both *in vitro* and *in vivo* diffuse by what is known as the free area theory. According to this theory, individual lipids move randomly to available open spaces within the

plane around each lipid. These open spaces are caused by the movement of other lipids within the membrane allowing for general mobility for the bilayer (Almeida et al., 2005; Vaz et al., 1984). This theory has been tracked and confirmed in model membranes through varying techniques (Lee et al., 1991; Sonnleitner et al., 1999). Even small changes in this random lipid diffusion can therefore theoretically reveal changes in membrane fluidity (Saffman & Delbruck, 1975). Additionally, transmembrane movement of lipids between the inner and outer leaflet of membrane has been revealed but the exact nature remains of how this mechanism occurs remains at the theoretical level (van Meer et al., 2008). Thus, the tracking individual lipid movement to elucidate mechanisms of individual lipid and microdomain activity remains a delicate process requiring great precision.

Total Internal Reflection Fluorescence (TIRF) studies have proven to be a successful method for the study of fluorescently tagged molecules within a SLB. TIRF utilizes an incoming laser reflected through a prism to create an evanescent field associated exclusively with the planar surface of a slide. The location of fluorophores within or attached to the surface can be found by tracking the areas of peak intensity. The exponential decrease of intensity from the location of the fluorescing substrate allows for extremely accurate tracking of the individual molecules (Axelrod, 2001). TIRF microscopy (TIRFM) has been widely used with planar supported membranes to study the translational diffusion of individual lipids, proteins, and other macromolecules located within the membranes themselves (Thomson et al., 1993).

The use of TIRFM to track individual molecules binding to integral membrane proteins already within the membrane has been largely through either fluorescence photobleaching recovery studies (TIR-FPR) (more generally known as Fluorescence Recovery after Photobleaching (FRAP)) or Single Particle Tracking (SPT). TIR-FPR involves the use of brief

heightened excitation of a portion of the membrane and the study of how fast the photobleached region recovers uniformity with the surrounding area (Huang et al., 1994; Thomson, et al., 1993). While TIR-FPR can elucidate changes in diffusion through bulk effects within the membrane, the study of individual interactions requires the use of SPT. SPT involves the tracking of an individually labeled protein or lipid through estimation of mean square displacement (*MSD*) of the fluorescing molecule between individual frames taken within a movie of the membrane (Qian et al., 1991; Saxton & Jacobson, 1997; Schütz et al., 1997). The diffusion coefficient (*D*) according to normal diffusion is then calculated by the equation:

$$D = \frac{MSD}{4t}$$

where *t* is time measured in seconds. As the diffusion coefficient illustrates the speed by which lipids move through the membrane, measurement of the diffusion coefficient before and after exposure of a SLB to interacting proteins can allow for the determination of membrane-protein interaction (Saxton & Jacobson, 1997). TIRF studies of interactions between proteins outside a model membrane and individual lipids within a SLB have not been recorded in the literature.

Another method utilizing diffusion coefficients to track both model membranes and molecules in solution is Fluorescence Correlation Spectroscopy (FCS). FCS involves the use of a laser to excite a specific spot of a fluorescently labeled sample. The laser is focused to create a small excitation volume during which any given time a number *N* molecules may be within the excitation volume. If *N* is relatively small it fluctuates stochastically because of diffusion and any fluctuations in *N* (or in fluorescence for a fluorescently labeled sample) can then be determined by the autocorrelation function of the fluorescence intensity according to a time  $\tau$ . This function for objects moving in three dimensions is given by the equation:

$$G(\tau) = 1 + \left[ \frac{\gamma}{N} \right] \times \left[ \frac{1}{1 + (\tau/\tau_R)} \right] \times \left[ \frac{1}{1 + (\omega_0/z_0)^2 \times (\tau/\tau_R)} \right]^{1/2}$$

where  $\tau$  is time,  $\gamma/N$  is a corrected value based on the inverse of the number  $N$  of molecules in the area,  $\omega_0$  is the lateral area measured,  $z_0$  is the axial length measured, and  $\tau_R$  is the time the molecule spends in the measured area (the residence time). Lipids and other components within a lipid bilayer move in two dimensions and thus the autocorrelation function becomes:

$$G(\tau) = 1 + \left[ \frac{\gamma}{N} \right] \times \left[ \frac{1}{1 + (\tau/\tau_R)} \right]$$

as  $\omega_0/z_0$  goes to infinity. The slower the species diffuse, the slower the decay in the correlation function. Thus, FCS can be used to determine diffusion coefficients of species in solution and the formula for this calculation from the residence time found by the autocorrelation function is:

$$D = \frac{\omega_{xy}^2}{4\tau_R}$$

where  $D$  is the diffusion coefficient,  $\omega_{xy}^2$  is the horizontal area of the volume observed, and  $\tau_R$  is the residence time (Korlach et al., 1999). However, first the volume of label within this spot and the label's random movements must be calibrated into the model by using reference lateral diffusion coefficients. FCS thus has great sensitivity for changes in molecular diffusion in the x and y directions of the plane for bulk assays (Benda et al., 2003; Machán & Hof, 2010).

The use of single molecule and bulk fluorescence studies on protein-lipid relationships is a relatively new development. Both TIRFM and FCS have been used successfully in the past to study interactions of lipids with both integral membrane proteins and free proteins within the cytosol. Much of the successful studies involving interactions with free proteins have been

studies of the acidic protein myristoylated alanine-rich C-kinase substrate (MARCKS) and its ability to sequester the basic lipid Phosphatidylinositol 4,5-bisphosphate (PI(4,5)P<sub>2</sub>) into lipid rafts through direct electrostatic interactions (Gambhir et al., 2004; Knight & Falke, 2009; Rusu et al., 2004). These studies have illustrated the possible avenues for success in *in vitro* fluorescence studies of interactions which have previously only been determined hypothetically via genetic mutation or conclusions from X-ray crystallography. This type of research may have special application for the study of vesicle guidance through adapter protein complexes.

### **Adapter Complexes**

After they were first characterized, different Adapter-related Protein Complexes (APs) were hypothesized to be associated with nearly every vesicular pathway within the cell because of their relation with the “clathrin cage” (M. Robinson, 1991). The protein clathrin was already known as the main component of the coat required in the formation of vesicles from biological membranes (Ungewickell & Branton, 1981). To solve the problem of how to sort vesicles within the cell, coat protein “adaptors” had been hypothesized and shortly thereafter isolated as “assembly polypeptides” (Pearse & Bretscher, 1981; Zaremba & Keen, 1983). Alpha-adaptin, later renamed AP-2, was found to be necessary for endocytosis (including at the neuronal synapse) and Beta-adaptin (AP-1) was revealed to be related to endosomal trafficking from the Trans-Golgi Network (Keen, 1990). Two further APs, AP-3 and AP-4, were later characterized by looking for structures similar to the previously discovered adaptins and both have been associated with post Golgi-apparatus endosomal sorting (M. S. Robinson, 2004).

All four known APs share a similar structure. They are heterotetramic, consisting of two large subunits (an entirely AP specific protein and a  $\beta$  subunit), a medium sized  $\mu$  subunit, and a small  $\sigma$  subunit. The  $\beta$ ,  $\mu$ , and  $\sigma$  subunits vary slightly between APs (Bonifacino & Dell'Angelica, 1999). The two large subunits both have a “head” and “ear” domain each, with the head facing the lipid membrane and the ear domain pointing away from the membrane (Hirst & Robinson, 1998). It has been shown that when forming the clathrin cage, the adaptin specific head domains of AP-2 and AP-1 ( $\alpha$  and  $\gamma$ , respectively) bind to highly charged lipids within a biological membrane while the ear domains of the  $\beta$  subunit bind clathrin (Slepnev & De Camilli, 2000; Wenk & De Camilli, 2004). AP-2 binds PI(4,5)P<sub>2</sub> within the cell membrane and AP-1 binds Phosphatidylinositol 4-phosphate (PI4P) within the Golgi Complex (Traub, 2003; Wang et al., 2003). The interactions of AP-3 and AP-4 with biological membranes when sorting membranes into vesicles have not been as well characterized.

AP-3 is the most well described adapter complex whose specific sorting machinery remains a mystery. AP-3's structure contains a  $\sigma_3$  subunit of approximately 22 kD, a 47 kD  $\mu_3$  subunit, a 120 kD  $\beta_3$  subunit, and an AP-3 specific 160 kD  $\delta$  subunit (Simpson et al., 1997). There are two primary forms of AP-3, neuronal and non-neuronal. The two differ structurally in their  $\beta_3$  and  $\mu_3$  subunits, but their primary differences are functional (Figure 1). Non-neuronal AP-3 is ubiquitous and responsible for some of the formation of lysosomes from endosomes throughout the body. Neuronal AP-3 is localized only to neuronal tissue. It is less well characterized, but likely responsible for the formation of synaptic vesicles from larger endosomes in neurons (Faundez, et al., 2007). AP-3 differs from AP-1 and AP-2 in that it may not necessarily require clathrin at all for its role in the formation of vesicles, though it still may

use clathrin in some circumstances (Dell'Angelica et al., 1998). However, of main interest for the study of AP-3 in model systems is its possible association with basic lipids.

AP-3 has been hypothesized to interact with PI4P when coordinated with a lipid membrane in the formation of vesicles. Phosphatidylinositol 4 kinase II alpha (PI4KII $\alpha$ ), which makes PI4P from regular phosphatidylinositol, has been found to be co-localized with AP-3 in rats through immunohistochemical labeling of the two proteins (G. Salazar et al., 2005). Additionally, blocking PI4KII $\alpha$  translation in rats with siRNA has been shown to prevent AP-3 from forming vesicles. As first hypothesized by Craige et al. (2008), AP-3 on an endosome may interact with residues in nearby PI4KII $\alpha$  to cause a local increase in PI4KII $\alpha$  which causes a microdomain of PI4P to develop and further recruit AP-3 to the membrane, thus eventually coming together to create a vesicle from the endosomal membrane. If this hypothesis were true, it would be likely that AP-3 interacts with PI4P in a similar manner to AP-1, binding PI4P when creating a vesicle. Thus, blocking PI4P production disallows the production of AP-3 vesicles even with AP-3. If the binding were similar to other adaptor complexes, then it would occur at the  $\delta$  subunit, which is conserved between both neuronal and non-neuronal AP-3 (Faundez, et al., 2007). However, this hypothesized interaction has not been proven through direct observation as of yet.

Reported here is an attempt to apply single molecule and bulk fluorescence microscopy to confirm the hypothesis that proteins such as AP-3 bind lipids (PI4P for AP-3) in a way that can be tracked utilizing fluorescence techniques. To observe this interaction, fluorescently tagged lipids were tracked utilizing three methods: (1) TIRFM for SPT of individually tagged PI4P and PI(4,5)P<sub>2</sub> (as a control and alternate hypothesis if AP-3 did not bind to PI4P) in order to record diffusion coefficients of SLBs before and after the introduction of AP-3. A control

model involving interactions between streptavidin and biotinylated lipids was established to evaluate the feasibility of tracking a protein-lipid interaction by evaluation of SPT for diffusion coefficients (Figure 2). (2) FCS of tagged lipids (RhPE, PI4P, biotin capped) both within solution and within an SLB to determine changes in diffusion after protein binding. (3) Immobilization of AP-3 to a slide through antibodies attached to the quartz and then tracking of interactions with water soluble fluorescently tagged PI4P. High affinity interactions would reduce the number of PI4P in solution because of binding to protein and be easily revealed by TIRFM. A positive result would yield a change in diffusion coefficient for TIRFM as well as FCS experiments and bound PI4P for the AP-3 immobilization experiments. A negative result would yield no changes in diffusion coefficient and no PI4P binding to immobilized AP-3.

## **Materials and Methods**

### **Lipid Materials**

Zwitterionic (and therefore overall neutral) lipids used were 1,2-dioleoyl-*sn*-glycero-3-phosphocholine (DOPC), 1-palmitoyl-2-oleoyl-*sn*-glycero-3-phosphocholine (POPC), 1,2-di-(9*Z*-octadecenoyl)-*sn*-glycero-3-phosphoethanolamine-N-(cap biotinyl) (Biotin PE), and L- $\alpha$ -Phosphatidylethanolamine-N-(lissamine rhodamine B sulfonyl) (RhPE) (purchased from Avanti Polar Lipids, Alabaster, AL). Fluorescently tagged phosphatidylinositol lipids were purchased from Echelon Biosciences (Salt Lake City, Utah) and included GloPIPs BODIPY TMR Phosphatidylinositol 4-phosphate (PI4P) and GloPIPs BODIPY TMR Phosphatidylinositol(4,5) biphosphate-C16 (PI(4,5)P2-C16) (Figure 3). Lipids were stored in chloroform at -4 °.

### **AP-3 purification**

AP-3 and other necessary proteins were purified via methods already in use (Gloria Salazar et al., 2004; Gloria Salazar et al., 2009). AP-3 was directly purified from rat brain cytosol obtained from Sprague-Dawley rats and stored at  $-80^{\circ}\text{C}$  (Clift-O'Grady et al., 1998; Desnos et al., 1995). AP-3 complexes were purified by immunoaffinity chromatography from the diluted RBC, and samples of AP-3 were subjected to immunoaffinity chromatography with AP-3 (mAb SA4) antibodies bound to Dynal M450 magnetic beads. Binding was performed for 3 hours at  $4^{\circ}\text{C}$ . Beads were washed six times in buffer A (10 nM HEPES, 150 nM NaCl, 1nM EDTA, and 0.1  $\text{MgCl}_2$  at pH 7.4) plus Triton X-100 0.1%. Afterwards beads were washed twice in buffer A in the absence of detergents. AP-3 complexes were eluted with a 50 micromolar concentration of a peptide corresponding to the epitope recognized by the anti- SA4 monoclonal antibody which corresponded to the amino acids 680–710 of human  $\alpha$ -adaptin. Elution was performed for two hours at  $0^{\circ}\text{C}$ . Complex purity was then confirmed by SDS-PAGE and protein concentration determined. Protein concentration was estimated at 10 ng/100 $\mu\text{L}$  buffer, or  $\sim 0.3$  nM.

### **Slides**

The quartz slides used were modified to make a chamber through which solutions could be flown. To make these chambers, a cover slip and quartz slide were fixed together by double-sided tape. The slides were of dimensions of  $5 \times 20 \times 0.1 \text{ mm}^3$  with two 1 mm diameter holes drilled into the slide for buffer exchange within the chamber. Buffer was thrown through the chamber before experimentation and then the chamber's edges were epoxied together to make it air-tight.

Slides were cleaned after experimentation to produce surfaces as clear of contamination as possible. Slides were sonicated in series with detergent (15 minutes), nanopure water (5 minutes), then rinsed with ethanol, rinsed with nanopure water, sonicated in acetone (10 minutes), rinsed with water, sonicated in water (5 minutes), rinsed, sonicated in 1 M KOH (20 minutes), rinsed, dried by nitrogen gas, burned, and rinsed/dried again before the coverslip was placed to remake the chamber. Fresh coverslips were sonicated for 20 minutes in 1 M KOH and rinsed/dried before being placed on the slide.

### **SUV Formation**

Small unilamellar vesicles (SUVs) were formed utilizing methods already well established (Barenholz, et al., 1977). Lipids were measured out and placed into glass tubes at the desired concentrations. These lipid mixtures were then evaporated under nitrogen gas until a thin lipid cake was visible around the bottom of the tube. They were then stored overnight under a vacuum. Afterwards, the lipids were resuspended in a filtered buffer containing 20 mM HEPES and 100 mM KCL (pH 7.2) at 65°C (because of the elevated transition temperature of saturated PIPs) to form multilamellar vesicles (MLVs). This MLV solution was then subjected to three freeze-thaw cycles consisting of 5 minutes in liquid nitrogen and 25 minutes in an incubator at 65°C. The MLV solution was then sonicated in a G112SP1 Special Ultrasonic Cleaner (Laboratory Supplies Co., Inc., Hicksville, NY) until clarity to produce small unilamellar vesicles (SUVs).

### **SLB formation**

SUVs were flown directly onto a quartz slide to create a solid-supported lipid bilayer (SLB) by vesicle fusion within two days of SUV formation. The bilayer was given thirty

minutes to form before being washed with buffer to remove excess lipids not within the SLB (Figure 4).

### **Biotinylated SLBs**

Biotinylated SLBs (in ratio of 1% Biotinylated PE to DOPC) required streptavidin and labeled biotinylated DNA binding before imaging could be performed. After the SLB was formed, the slide was imaged to check for background. Then streptavidin was then added at high enough concentration to cover the slide and given 10 minutes to bind the biotinylated PE. After washing, Cy3 labeled biotinylated DNA was added at variable concentrations (typically 1 or 10 nM) and given 5 minutes to bind to streptavidin before another round of washing (Figure 4). Imaging with Cy3-labeled DNA required a saturated Trolox imaging buffer to prevent blinking and limit photobleaching.

### **TIRFM**

TIRFM was performed utilizing a home-made TIR microscope with a Charged Coupled Device (CCD) camera which has proven accurate in single molecule studies (Rasnik et al., 2004). The inverted microscope (IX71, Olympus) imaged a  $50\ \mu\text{m} \times 100\ \mu\text{m}$  area to the camera. Fluorescent molecules within the chamber were excited using a Nd:YAG laser (532 nm, Crystalaser, power 10–20 mW at the sample plane) through a quartz prism placed over the quartz slide with a thin layer of immersion oil in between. The incident angle of the laser was controlled to achieve total internal reflection at the interface between the quartz slide and aqueous buffer. Fluorescently labeled lipids within the solid-supported lipid bilayer were by nature attached to this interface and background fluorescence arising from the fluorescent molecules in solution was minimized as excitation intensity decayed exponentially from the interface. Fluorescence

signal was collected using a water immersion objective (Olympus; 60 $\times$ , 1.2 numerical aperture). After rejecting the scattered laser light using a long pass interference filter at 550 nm (Chroma), the imaging area was defined using a vertical slit located at the imaging plane of the microscope just outside the left side port. The emission was subsequently collimated using a 12 cm focal length achromat lens (Oriel), split by a long pass extended reflection dichroic mirror at 635 nm (Chroma), recombined using an identical dichroic mirror after reflecting off a mirror each, and finally imaged onto the CCD camera using a 24 cm focal length achromat lens (Oriel) to achieve 2 $\times$  magnification for video (Figure 6).

## **FCS**

Single-photon FCS was utilized to study the lipid dynamics of water-soluble lipids (labeled PI4P and RhPE) and lipids within a SLB. The system was calibrated with Rhodamine 6G as its known species. 100  $\mu$ L solutions were prepared and flown into slides before being imaged. A IX51, Olympus microscope was utilized for the objective. Various solution molarities were utilized depending on the interaction being studied. Light coming through the sample passed through a filter to reduce background and a lens to focus the image before passing through a slit to the Avalanche Photodiode which counted the fluorescence within the excited area (Figure 7).

## **Viscosity Tests of Biotinylated SLBs**

To tests for the effects of buffer viscosity on the mobility of streptavidin bound-biotinylated lipids, various percentages of sucrose were added to the 25 mM HEPES, 100 mM KCl buffer in the presence of saturated Trolox. 0%, 10%, 20%, 30%, 40%, and 50% sucrose buffers were utilized. Each sucrose solution was exposed to a single slide with a made

streptavidin bound-biotinylated SLB in succession. 200  $\mu$ L of each sucrose solution was flown through the slide three times and left for ten minutes to assure effects noticed were for a solution of the proper concentration. The slide was then subjected to FCS for calculation of the fluorescence correlation curve and diffusion coefficient analysis before another solution was added. The protocol was repeated for a 0.01% RhPE labeled lipid bilayer as a control for a non-streptavidin bound bilayer. Another control with just Rhodamine 6G (just the dye with no lipid bound) in solution was tested by FCS to compare SLB effects of viscosity on a freely moving substrate not constrained to a bilayer with the SLB FCS data.

### **AP-3 Immobilization**

To test that undiluted PI4P with a six carbon chain tail (the one utilized in this study) existed as a free lipid within solution and did not spontaneously form a micelles or vesicles, PI4P in solution was compared to water-soluble Rhodamine 6G by FCS.

The immunoglobulin binding protein G was utilized for AP-3 immobilization directly onto the quartz slides. A 0.5 mg/mL solution of protein G (in buffer A) was flown through the chamber and incubated for 20 minutes for binding of the protein onto the slide. After incubation, buffer A was flown through the chamber to remove excess protein G. A Bovine Serum Albumin (BSA) solution (0.5 mg/mL) was then flown through the chamber to fill areas of the quartz not bound by protein G in an effort to avoid nonspecific binding and given ten minutes for incubation. After removing excess BSA with buffer A, mAb anti-delta SA4 antibodies specific for AP-3 were flown through the slide at a concentration of 10 nM and given 10 minutes to incubate before being washed away with buffer to remove excess antibodies. Rat brain cytosol was then directly flown onto the slide and incubated for three hours to allow for the binding of

AP-3 to the antibodies. After incubation and washing, a variable solution of PI4P (1 nM, 10 nM, 50 nM, 100 nM) was flown through the slide and immediately imaged by TIRFM. The total number of labeled species in the area was counted over 500 frames and compared to the number of labeled PI4P counted on a control slide. This control slide contained bound H4A3 (a monoclonal antibody for the human protein LAMP1), which should not have bind any proteins within the RBC and thus served as a control nonspecific binding of AP-3 (Figure 8).

As a further control for the possibility of nonspecific binding to the glass via electrostatic interaction, a directly labeled antibody was tested. This Texas Red tagged antibody was used to compare binding to the slide with and without the addition of Protein G in the protocol (Figure 9). Antibodies were obtained from the Developmental Studies Hybridoma Bank (Iowa City, IA).

### **Data Analysis**

Data was analyzed via Labview® computer software (National Instruments Co. Austin, TX) commonly used for fluorescence spectroscopy. This software allowed for SPT through the determination of trajectories for individual particles from the movies obtained with the CCD camera of the TIR microscope. Diffusion coefficients were calculated from the data to determine changes in mass associated with molecular alterations. The same computer software was utilized to compile FCS data and determine the fluctuations in the fluorescence signal for the determination of the correlation function for the fluorescence, from which it was possible to obtain the diffusion coefficient. Raw data from Labview was analyzed with OriginLab® graphing and data analysis software (Origin Lab Co. Northampton, MA).

### **Results**

#### **TIRFM of Biotinylated Bilayers**

TIRFM of the model biotin/streptavidin system illustrated a decrease in the mobility of the membrane after streptavidin binding to the biotinylated membrane compared to SLBs composed of a similar visible percentage of fluorescently tagged lipids (head-labeled RhPE) (Figure 9). This decrease was visible to the eye. SPT of these membranes revealed a drop in the diffusion coefficient from  $1.94 \times 10^{-8} \text{ cm}^2/\text{s}$  for the RhPE labeled bilayer to  $1.17 \times 10^{-8} \text{ cm}^2/\text{s}$  for the biotinylated system (Figure 11).

### **FCS of Biotinylated Bilayers and Effects of Viscosity**

FCS of the model biotin/streptavidin system showed a similar 50% drop in the diffusion coefficient when compared to RhPE labeled SLBs by FCS at 0% sucrose (the same buffer as utilized in the above TIRFM experiment). Increases in viscosity produced decreases in the diffusion coefficient, reaching about a 4x decrease in diffusion at 50% sucrose for the biotin/streptavidin system. No change in diffusion coefficient with increased buffer viscosity was evident for the RhPE labeled SLB. This contrasted significantly with Rhodamine 6G in solution, which had a linear relationship with increased viscosity (Figure 12).

### **TIRFM of PIP systems with and without AP-3**

Attempts to make SLBs containing PI4P and PI(4,5)P2 in DOPC and POPC bilayers produced bilayers of limited mobility. A large immobile fraction was typically present and aggregates were common. This made diffusion coefficient tracking by SPT impossible by TIRFM. The introduction of 0.3 nM AP-3 (the concentration of the purified RBC) into the system produced no visible changes in labeled PI4P diffusion within the imaged areas viewed at 0, 1, and 3 hours of incubation. Additionally, no changes in numbers or sizes of aggregates were visible (Figure 13).

### **FCS of PI4P, RhPE**

FCS of low volumes of PI4P and Rhodamine 6G in solution illustrated a 30% drop in the diffusion coefficient from Rhodamine to PI4P. This was in good agreement with the expected dependence of the diffusion coefficient with the cubic root of the molecular weight as the molecular weights of PI4P and Rhodamine 6G are 1200 Da and 500 Da, respectively (Figure 14). These values indicated that PI4P was soluble in solution as micelles or vesicles would have yielded a much smaller diffusion coefficient.

### **Nonspecific Binding Check for Antibody Immobilization**

Antibody immobilization utilizing Protein G proved to be very specific. When viewed by TIRFM, Texas Red antibodies appeared in high numbers in the presence of Protein G but did not when Protein G was absent. While labeled antibody was still evident, the differences between the two scenarios were large enough that nonspecific binding was considered inconsequential. No fluorescence was visible in the absence of labeled antibody (Figure 15).

### **AP-3 binding with Antibodies**

No discernable differences were noted between the mAb anti-delta SA4 and H4A3 bound slides. The average of 500 frames of data from movies of each illustrated a similar number of mobile PI4P molecules for the two antibodies (Figure 16). When the cumulative number of molecules for the entire movies was plotted versus time it was found that this similarity in numbers of mobile PI4Ps was constant for the entire period (Figure 17). Thus the number of bound PI4Ps would have been the same for both slides and it is even possible that no PI4Ps in the solution were bound at all in either case.

## **Discussion**

### **TIRFM and FCS of Biotinylated SLB**

The evident drop in diffusion coefficient in the streptavidin/biotinylated SLB systems evident under both single molecule (SPT) and bulk (FCS) techniques provide relative certainty to protein binding's constraining effect on lipid mobility. The nearly identical drop in the diffusion coefficient (around 50% for both) supports this assertion. This result was unexpected as the free area theory for lipid translational movement within the bilayer only poses random open space around the individual lipid as cause for lipid diffusion in the absence of integral membrane proteins, cholesterol, or other constraining molecules within the membrane. Thus another force not within the model is at work.

While streptavidin has four binding sites, protein binding to multiple lipids as the cause of this drop in mobility is unlikely. It only likely binds one biotinylated lipid in this system as only 1/100 lipids are biotinylated and not all streptavidin bound biotin was labeled with fluorescently tagged DNA in the system. Thus the odds of multiple bound biotinylated lipids per streptavidin are low (especially in the bulk FCS assay). Additionally, each streptavidin is likely not associating transiently and re-associated with another biotinylated lipid to form a microdomain of biotinylated lipids because the streptavidin-biotin interaction is extremely strong ( $K_d \sim 10^{-15}$ ).

The changes in diffusion coefficient with changes in buffer viscosity reinforce the idea of the streptavidin-biotin binding changing the nature of lipid movement in the bilayer. The overall effects of viscosity on a SLB are still debated in the literature (Sackmann, 1996). However, the data from FCS did not illustrate any discernable effects of increased viscosity on a directly

labeled membrane. Label in solution, however, was affected by viscosity in the linear fashion expected from known viscosity values (at 50% sucrose, Rhodamine 6G diffused 15 times slower) (Table 1). The streptavidin/biotinylated SLB proved to be a mixture of the two scenarios. Unlike a simple SLB, the diffusion coefficient dropped with increased viscosity (4x) but it did not change anywhere near as much as label in solution. This illustrates a direct effect of viscosity on the bound streptavidin, likely from friction from the buffer pushing on the protein and further preventing it from moving into an open space it would have before even with the protein bound to the functionalized lipid (Figure 18). This “drag” effect of bound protein to lipid has not been reported as a specific result of protein binding to lipids within the bilayer.

### **TIRFM of Labeled Phosphoinositides PI4P and PI(4,5)P2**

Labeled PI4P and PI(4,5)P2 proved to be problematic for study utilizing solid-supported lipid bilayers. The formation of aggregates despite in the absence of protein and the immobile fraction both represent an obstacle for study through SPT. SPT requires the ability to follow a labeled species continuously over a number of frames, but the combination of effects of the already formed aggregates and immobile fraction confounded any results obtained. Additionally, the fast photobleaching of the BODIPY dyes made tracking an individual molecule over a long period of time highly problematic. A bulk study of these membranes through FCS may be more successful, but was not performed due to time constraints.

The primary problems for these bilayers were the aggregates. These aggregates may have formed for a number of reasons. First, it is currently a topic of debate as to whether highly charged PIPs form microdomains on their own through hydrogen bonding with other PIPs or the solution itself (Fernandes et al., 2006; Gambhir, et al., 2004; Hermelink & Brezesinski, 2008;

Redfern & Gericke, 2004). Additionally, it is possible that neither the PI4P utilized with its six carbon long acyl-chain nor the PI(4,5)P2 used with its sixteen carbon long acyl-chain were stable within the model membrane and may have diffused out of the membrane (Cho et al., 2006). However, the mobile fraction likely illustrated that some mixing of PC and labeled PIPs did occur and at times even RhPE formed aggregates in SLBs for unknown reasons.

### **TIRFM of AP-3 and Labeled PI4P**

TIRF imaging of AP-3 interactions with a labeled PI4P did not yield any visible changes in bilayer mobility. While the above problems listed may have been major factors in this, the primary difficulty with the experiment was the amount of AP-3 purified from the RBC. At its highest purity and highest yield, the method only yielded a concentration less than 0.3 nM of AP-3 as measured by SDS-PAGE. Even single molecule experiments require at least nanomolar concentration to detect very high affinity binding and likely AP-3 does not bind PIPs with such high affinity. Producing solutions with greater concentrations of AP-3 required purification and protein synthesis techniques which were outside of the time constraints of this study.

### **AP-3 Immobilization**

While the Texas Red antibody assay showed that nonspecific binding appeared to be negligible for the immobilization system, the test for AP-3 binding did not yield clear results. The lack of a difference between the AP-3 binding anti-delta SA4 antibody and H4A3 antibody experiments could have been for one of three reasons. The first is the same as the likely issue with the TIRFM experiments. While RBC was flown directly onto the slide to bind antibody directly on the slide and therefore should have attached more AP-3 to the slide than the elution process produced, it is unknown still if this produced enough immobilized AP-3 to show binding.

In fact, the second possible cause of failure for this system to show PIP binding is that it is unknown if the AP-3 even bound to the immobilized antibody at all. Without a tag for the protein or a tagged antibody to bind AP-3, this proved impossible to confirm. Finally, the experiment may have gone perfectly and just illustrated a negative result (AP-3 does not bind PI4P). However, without being able to refute the first two possibilities it was impossible to be certain of this result.

### **Conclusions**

Fluorescent microscopy techniques proved to be a useful tool for the study of protein-lipid binding. By far the most intriguing of the results was the drag effect of streptavidin binding on biotinylated lipids as revealed by SPT and FCS. This effect is not accounted for in the current model for lipid movement within the bilayer and therefore may have great implications for future study of protein-membrane binding. Further studies on this interaction with labeled lipids and proteins with known lipid binding (such as labeled PI4P and proteins known to bind PI4P) should be done to corroborate this interaction outside the streptavidin/biotin system. If confirmed, an adapted model of the free area theory when bound by proteins on one side of the membrane surface will have to be made.

The TIRF and immobilization analysis of AP-3, on the other hand, did not reveal any significant conclusions on AP-3's binding of PI4P or PI(4,5)P2. At best, this study illustrates a negative result of PIPs not binding directly with AP-3. Repetition of these studies with significantly larger concentrations of AP-3 and more work on lipid mixing within the bilayer will be necessary before any final analysis of this interaction can be made. Additionally, a control system of labeled PIPs within a SLB interacting with a protein of known PIP binding will be

necessary to confirm the technique. Still, this study provides a basis for further research on direct observation of protein-lipid interactions on the surface of model lipid membranes, a subject with great implications on intracellular communication and other necessary biological activities.

## References

- Almeida, P. F., Vaz, W. L., & Thompson, T. E. (2005). Lipid diffusion, free area, and molecular dynamics simulations. *Biophys J*, 88(6), 4434-4438.
- Axelrod, D. (2001). Total Internal Reflection Fluorescence Microscopy in Cell Biology. *Traffic*, 2(11), 764-774.
- Barenholz, Y., Gibbes, D., Litman, B. J., Goll, J., Thompson, T. E., & Carlson, R. D. (1977). A simple method for the preparation of homogeneous phospholipid vesicles. *Biochemistry*, 16(12), 2806-2810.
- Benda, A., Beneš, M., Mareček, V., Lhotský, A., Hermens, W. T., & Hof, M. (2003). How To Determine Diffusion Coefficients in Planar Phospholipid Systems by Confocal Fluorescence Correlation Spectroscopy. *Langmuir*, 19(10), 4120-4126.
- Boggs, J. M. (1987). Lipid intermolecular hydrogen bonding: influence on structural organization and membrane function. *Biochimica et Biophysica Acta (BBA) - Reviews on Biomembranes*, 906(3), 353-404.
- Bonifacino, J. S., & Dell'Angelica, E. C. (1999). Molecular Bases for the Recognition of Tyrosine-based Sorting Signals. *J. Cell Biol.*, 145(5), 923-926.
- Cho, H., Kim, Y. A., & Ho, W. K. (2006). Phosphate number and acyl chain length determine the subcellular location and lateral mobility of phosphoinositides. *Mol Cells*, 22(1), 97-103.
- Clift-O'Grady, L., Desnos, C., Lichtenstein, Y., Faúndez, V., Horng, J.-T., & Kelly, R. B. (1998). Reconstitution of Synaptic Vesicle Biogenesis from PC12 Cell Membranes. *Methods*, 16(2), 150-159.
- Craige, B., Salazar, G., & Faundez, V. (2008). Phosphatidylinositol-4-Kinase Type II Alpha Contains an AP-3-sorting Motif and a Kinase Domain That Are Both Required for Endosome Traffic. *Mol. Biol. Cell*, 19(4), 1415-1426.
- Dell'Angelica, E. C., Klumperman, J., Stoorvogel, W., & Bonifacino, J. S. (1998). Association of the AP-3 Adaptor Complex with Clathrin. *Science*, 280(5362), 431-434.
- Desnos, C., Clift-O'Grady, L., & Kelly, R. B. (1995). Biogenesis of synaptic vesicles in vitro. *J Cell Biol*, 130(5), 1041-1049.
- Edidin, M. (1997). Lipid microdomains in cell surface membranes. *Current Opinion in Structural Biology*, 7(4), 528-532.

- Edidin, M. (2003). The State of Lipid Rafts: From Model Membranes to Cells. *Annual Review of Biophysics and Biomolecular Structure*, 32(1), 257-283.
- Faundez, V., Seong, E., Burmeister, M., & Newell-Litwa, K. (2007). Neuronal and non-neuronal functions of the AP-3 sorting machinery. *J Cell Sci*, 120(4), 531-541.
- Fernandes, F., Loura, L. M. S., Fedorov, A., & Prieto, M. (2006). Absence of clustering of phosphatidylinositol-(4,5)-bisphosphate in fluid phosphatidylcholine. *J. Lipid Res.*, 47(7), 1521-1525.
- Gambhir, A., Hangyas-Mihalyne, G., Zaitseva, I., Cafiso, D. S., Wang, J., Murray, D., et al. (2004). Electrostatic sequestration of PIP2 on phospholipid membranes by basic/aromatic regions of proteins. *Biophys J*, 86(4), 2188-2207.
- Hermelink, A., & Brezesinski, G. (2008). Do unsaturated phosphoinositides mix with ordered phosphadidylcholine model membranes? *J. Lipid Res.*, 49(9), 1918-1925.
- Hirst, J., & Robinson, M. S. (1998). Clathrin and adaptors. *Biochimica et Biophysica Acta (BBA) - Molecular Cell Research*, 1404(1-2), 173-193.
- Hofmann, G. (Ed.). (1977). *Iscotables* (7th ed.).
- Huang, Z., Pearce, K. H., & Thompson, N. L. (1994). Translational diffusion of bovine prothrombin fragment 1 weakly bound to supported planar membranes: measurement by total internal reflection with fluorescence pattern photobleaching recovery. *Biophys J*, 67(4), 1754-1766.
- Johnson, J. M., Ha, T., Chu, S., & Boxer, S. G. (2002). Early steps of supported bilayer formation probed by single vesicle fluorescence assays. *Biophysical Journal*, 83(6), 3371-3379.
- Keen, J. H. (1990). Clathrin and Associated Assembly and Disassembly Proteins. *Annual Review of Biochemistry*, 59(1), 415-438.
- Kleemann, W., & McConnell, H. M. (1976). Interactions of proteins and cholesterol with lipids in bilayer membranes. *Biochimica et Biophysica Acta (BBA) - Biomembranes*, 419(2), 206-222.
- Knight, J. D., & Falke, J. J. (2009). Single-molecule fluorescence studies of a PH domain: new insights into the membrane docking reaction. *Biophys J*, 96(2), 566-582.
- Korlach, J., Schwille, P., Webb, W. W., & Feigensohn, G. W. (1999). Characterization of lipid bilayer phases by confocal microscopy and fluorescence correlation spectroscopy. *Proc Natl Acad Sci U S A*, 96(15), 8461-8466.

- Lee, G. M., Ishihara, A., & Jacobson, K. A. (1991). Direct observation of brownian motion of lipids in a membrane. *Proceedings of the National Academy of Sciences of the United States of America*, 88(14), 6274-6278.
- Machán, R., & Hof, M. (2010). Lipid diffusion in planar membranes investigated by fluorescence correlation spectroscopy. *Biochimica et Biophysica Acta (BBA) - Biomembranes*, *In Press*, *Corrected Proof*.
- McConnell, H. M., Watts, T. H., Weis, R. M., & Brian, A. A. (1986). Supported planar membranes in studies of cell-cell recognition in the immune system. *Biochimica et Biophysica Acta (BBA) - Reviews on Biomembranes*, 864(1), 95-106.
- Nagle, J. F. (1980). Theory of the Main Lipid Bilayer Phase Transition. *Annual Review of Physical Chemistry*, 31(1), 157-196.
- Olson, F., Hunt, C. A., Szoka, F. C., Vail, W. J., & Papahadjopoulos, D. (1979). Preparation of Liposomes of Defined Size Distribution by Extrusion Through Polycarbonate Membranes. *Biochimica et Biophysica Acta*, 557, 9-23.
- Paolo, G. D., & Camilli, P. D. (2006). Phosphoinositides in cell regulation and membrane dynamics. *Nature*, 443, 651-657.
- Pearse, B. M. F., & Bretscher, M. S. (1981). Membrane Recycling by Coated Vesicles. *Annual Review of Biochemistry*, 50(1), 85-101.
- Qian, H., Sheetz, M. P., & Elson, E. L. (1991). Single particle tracking. Analysis of diffusion and flow in two-dimensional systems. *Biophysical Journal*, 60(4), 910-921.
- Rasnik, I., Myong, S., Cheng, W., Lohman, T. M., & Ha, T. (2004). DNA-binding Orientation and Domain Conformation of the E. coli Rep Helicase Monomer Bound to a Partial Duplex Junction: Single-molecule Studies of Fluorescently Labeled Enzymes. *Journal of Molecular Biology*, 336(2), 395-408.
- Redfern, D. A., & Gericke, A. (2004). Domain formation in phosphatidylinositol monophosphate/phosphatidylcholine mixed vesicles. *Biophys J*, 86(5), 2980-2992.
- Robinson, M. (1991). Membrane traffic COPS. *Nature(London)*, 349(6312), 743-744.
- Robinson, M. S. (2004). Adaptable adaptors for coated vesicles. *Trends in Cell Biology*, 14(4), 167-174.
- Rusu, L., Gambhir, A., McLaughlin, S., & Rädler, J. (2004). Fluorescence Correlation Spectroscopy Studies of Peptide and Protein Binding to Phospholipid Vesicles. *Biophysical Journal*, 87(2), 1044-1053.

- Sackmann, E. (1996). Supported Membranes: Scientific and Practical Applications. *Science*, 271(5245), 43-48.
- Saffman, P. G., & Delbruck, M. (1975). Brownian motion in biological membranes. *Proc Natl Acad Sci U S A*, 72(8), 3111-3113.
- Sako, Y., & Yanagida, T. (2003). Single-molecule visualization in cell biology. *Nat Rev Mol Cell Biol, Suppl*, SS1-5.
- Salazar, G., Craige, B., Wainer, B. H., Guo, J., De Camilli, P., & Faundez, V. (2005). Phosphatidylinositol-4-kinase type II alpha is a component of adaptor protein-3-derived vesicles. *Molecular Biology of the Cell*, 16(8), 3692-3704.
- Salazar, G., Love, R., Werner, E., Doucette, M. M., Cheng, S., Levey, A., et al. (2004). The Zinc Transporter ZnT3 Interacts with AP-3 and It Is Preferentially Targeted to a Distinct Synaptic Vesicle Subpopulation. *Mol. Biol. Cell*, 15(2), 575-587.
- Salazar, G., Zlatic, S., Craige, B., Peden, A. A., Pohl, J., & Faundez, V. (2009). Hermansky-Pudlak Syndrome Protein Complexes Associate with Phosphatidylinositol 4-Kinase Type II alpha in Neuronal and Non-neuronal Cells. *Journal of Biological Chemistry*, 284(3), 1790-1802.
- Saxton, M. J., & Jacobson, K. (1997). Single Particle Tracking: Applications to Membrane Dynamics. *Annual Review of Biophysics and Biomolecular Structure*, 26(1), 373-399.
- Schütz, G. J., Schindler, H., & Schmidt, T. (1997). Single-molecule microscopy on model membranes reveals anomalous diffusion. *Biophysical Journal*, 73(2), 1073-1080.
- Simons, K., & Ehehalt, R. (2002). Cholesterol, lipid rafts, and disease. *The Journal of Clinical Investigation*, 110(5), 597-603.
- Simpson, F., Peden, A. A., Christopoulou, L., & Robinson, M. S. (1997). Characterization of the Adaptor-related Protein Complex, AP-3. *J. Cell Biol.*, 137(4), 835-845.
- Singer, S. J., & Nicolson, G. L. (1972). The Fluid Mosaic Model of the Structure of Cell Membranes. *Science*, 175(4023), 720-731.
- Slepnev, V. I., & De Camilli, P. (2000). Accessory factors in clathrin-dependent synaptic vesicle endocytosis. [10.1038/35044540]. *Nat Rev Neurosci*, 1(3), 161-172.
- Sonnleitner, A., Schutz, G. J., & Schmidt, T. (1999). Free brownian motion of individual lipid molecules in biomembranes. *Biophys J*, 77(5), 2638-2642.

- Thomson, N. L., Pearce, K. H., & Hsieh, H. V. (1993). Total internal reflection fluorescence microscopy: application to substrate-supported planar membranes. [10.1007/BF00213560]. *European Biophysics Journal*, 22(5), 367-378.
- Tocanne, J.-F., Dupou-Cézanne, L., & Lopez, A. (1994). Lateral diffusion of lipids in model and natural membranes. *Progress in Lipid Research*, 33(3), 203-237.
- Traub, L. M. (2003). Sorting it out: AP-2 and alternate clathrin adaptors in endocytic cargo selection. *J. Cell Biol.*, 163(2), 203-208.
- Ungewickell, E., & Branton, D. (1981). Assembly units of clathrin coats. [10.1038/289420a0]. *Nature*, 289(5796), 420-422.
- van Meer, G., Voelker, D. R., & Feigenson, G. W. (2008). Membrane lipids: where they are and how they behave. *Nat Rev Mol Cell Biol*, 9(2), 112-124.
- Vaz, W. L. C., Goodsaid-Zalduondo, F., & Jacobson, K. (1984). Lateral diffusion of lipids and proteins in bilayer membranes. *FEBS Letters*, 174(2), 199-207.
- Veatch, S. L., & Keller, S. L. (2002). Organization in Lipid Membranes Containing Cholesterol. *Physical Review Letters*, 89(Copyright (C) 2010 The American Physical Society), 268101.
- Wagner, M. L., & Tamm, L. K. (2000). Tethered Polymer-Supported Planar Lipid Bilayers for Reconstitution of Integral Membrane Proteins: Silane-Polyethyleneglycol-Lipid as a Cushion and Covalent Linker. *Biophysical Journal*, 79(3), 1400-1414.
- Wang, Y. J., Wang, J., Sun, H. Q., Martinez, M., Sun, Y. X., Macia, E., et al. (2003). Phosphatidylinositol 4 Phosphate Regulates Targeting of Clathrin Adaptor AP-1 Complexes to the Golgi. *Cell*, 114(3), 299-310.
- Wenk, M. R., & De Camilli, P. (2004). Protein-lipid interactions and phosphoinositide metabolism in membrane traffic: Insights from vesicle recycling in nerve terminals. *Proceedings of the National Academy of Sciences of the United States of America*, 101(22), 8262-8269.
- Zaremba, S., & Keen, J. (1983). Assembly polypeptides from coated vesicles mediate reassembly of unique clathrin coats. *J. Cell Biol.*, 97(5), 1339-1347.
- Zhang, L., & Granick, S. (2005). Slaved diffusion in phospholipid bilayers. *Proceedings of the National Academy of Sciences of the United States of America*, 102(26), 9118-9121.

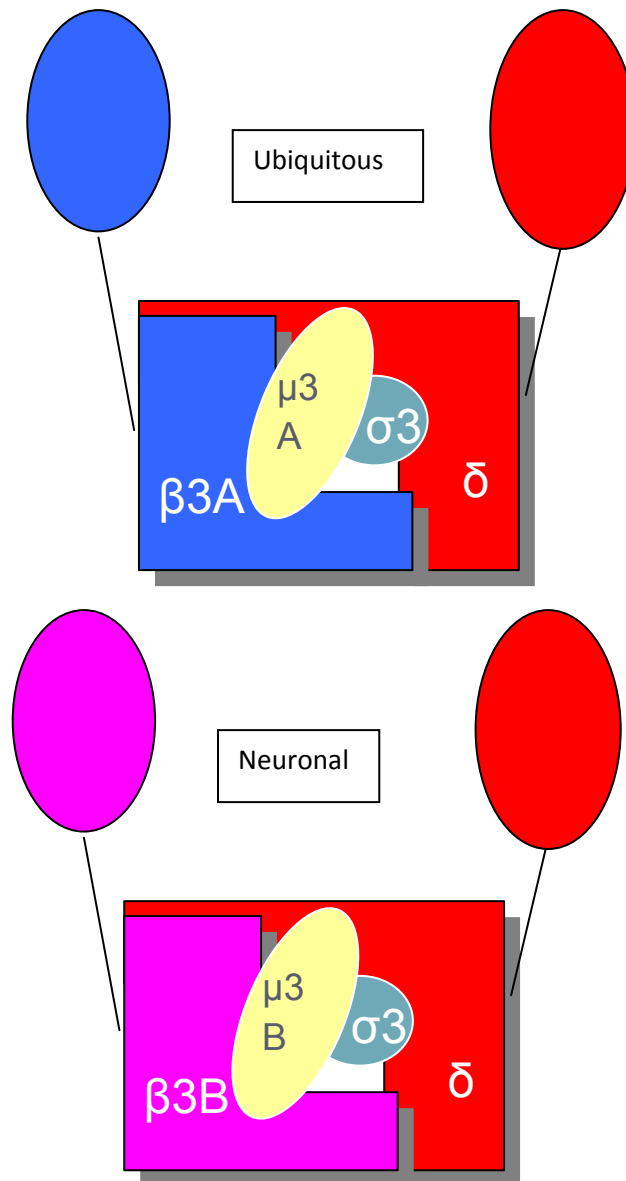


**Figure 1:** Schematics of Ubiquitous and Neuronal AP-3. The two differ in the  $\beta 3$  and  $\mu 3$  subunits. The  $\delta$  subunit is hypothesized to have lipid interactions.

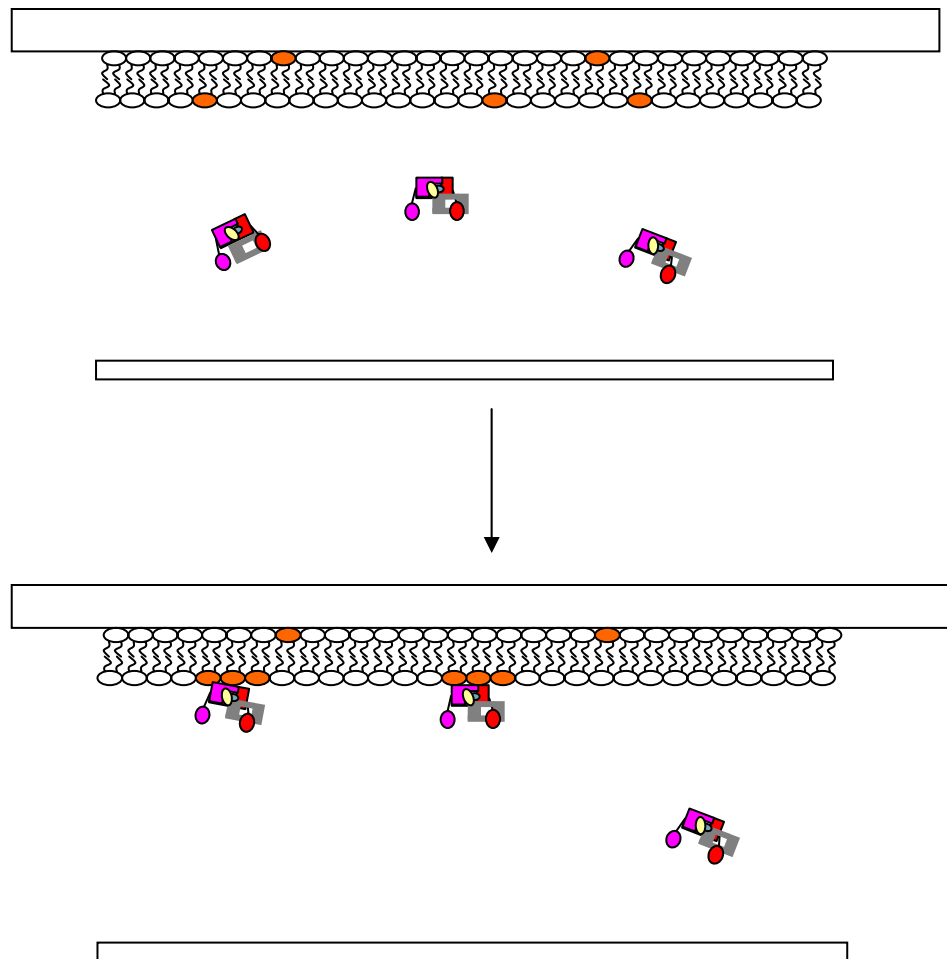


**Figure 2:** Theoretical depiction of AP-3 binding to tagged PI4P within a SLB and causing aggregates (lipid rafts) to form.

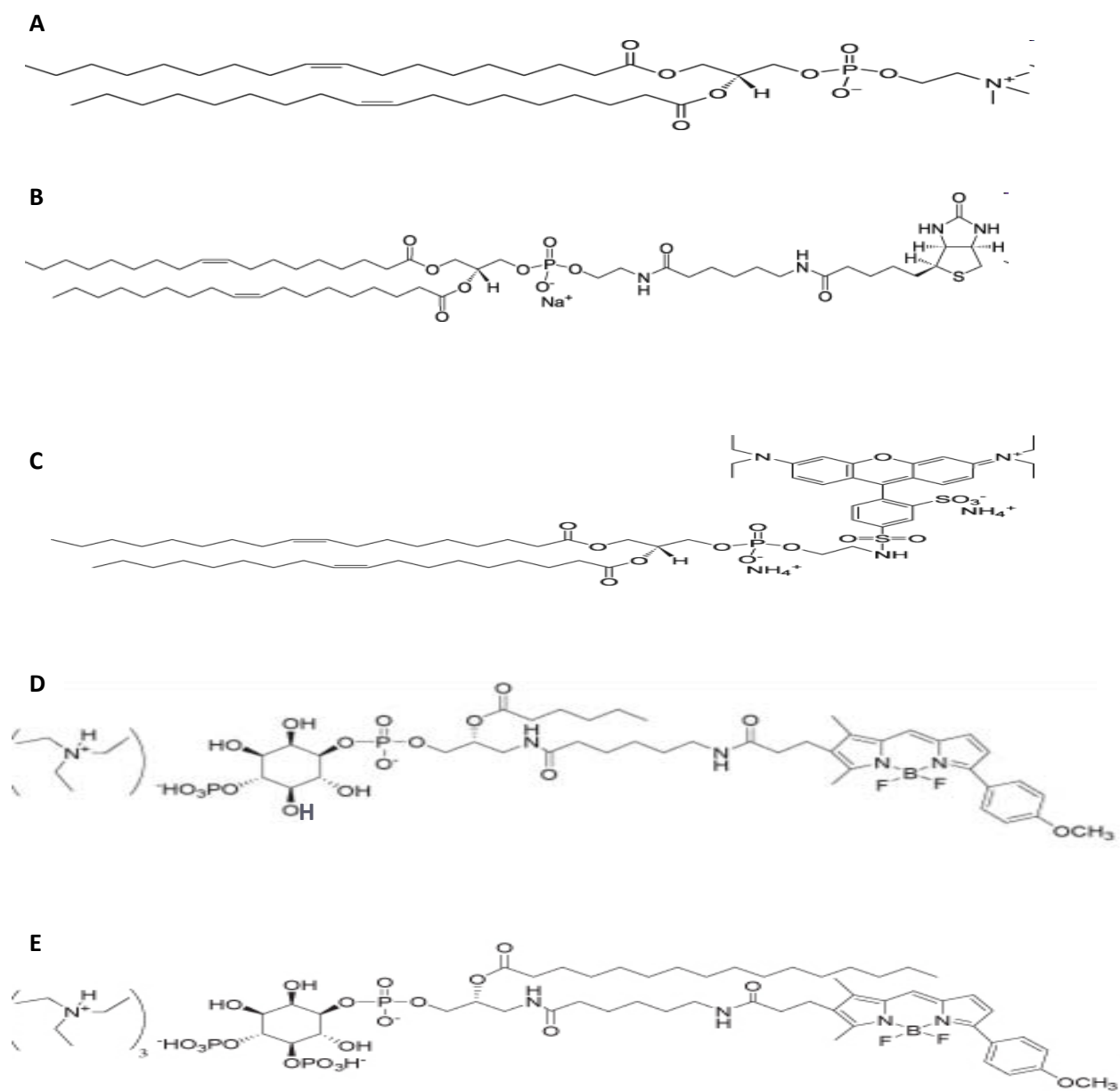


**Figure 3:** Molecular structures of lipids utilized in the study, including: (A) 1,2-di-(9Z-octadecenoyl)-sn-glycero-3-phosphocholine (DOPC); (B) 1,2-di-(9Z-octadecenoyl)-sn-glycero-3-phosphoethanolamine-N-(cap biotinyl) (Biotin capped PE); (C) L- $\alpha$ -Phosphatidylethanolamine-N-(lissamine rhodamine B sulfonyl) (RhPE); (D) GloPIPs BODIPY TMR Phosphatidylinositol 4-phosphate (PI4P); and (E) GloPIPs BODIPY TMR Phosphatidylinositol(4,5) bisphosphate-C16 (PI(4,5)P2).

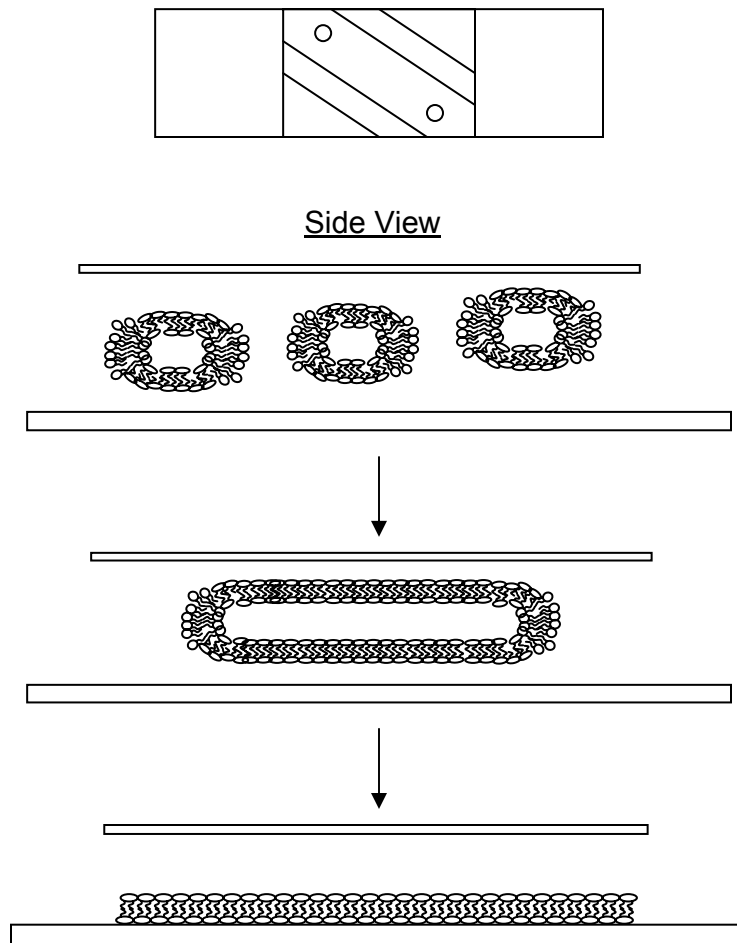


**Figure 4:** Schematic of slide setup. (A) A top view of a quartz slide w/cover slip chamber. (B) A side view of the formation of an SLB from SUVs. SUVs join together to form larger vesicles which, at high enough density, rupture in the presence of the quartz support and form the SLB.

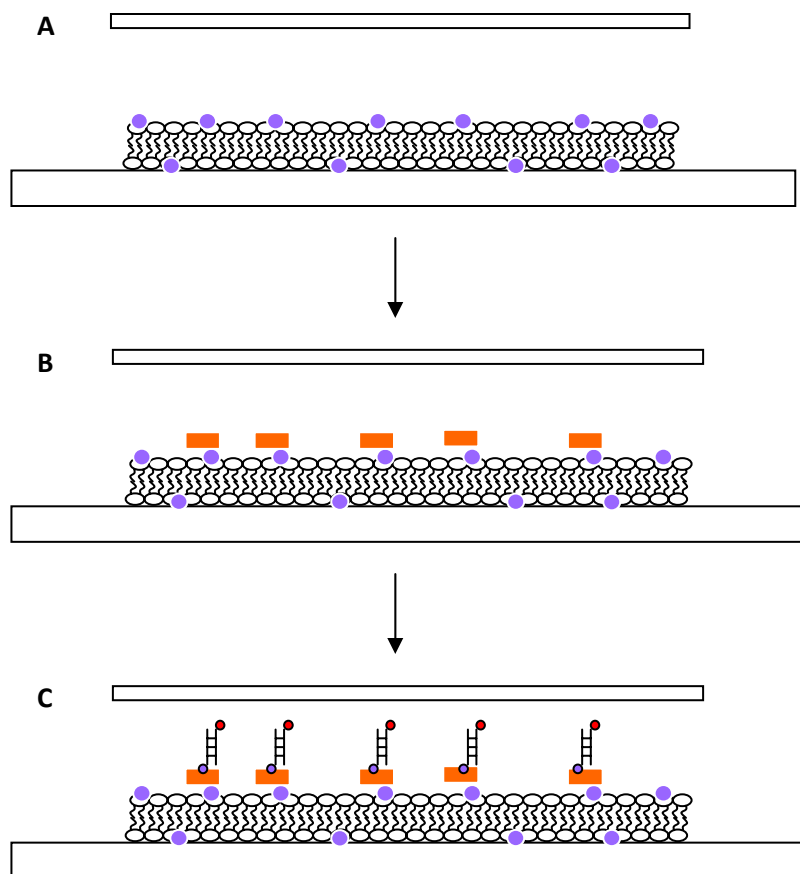


**Figure 5:** Drawing of Biotin model system. A biotinylated SLB (A) is exposed to streptavidin and the biotin and streptavidin bind with high affinity (B). Fluorescently labeled biotinylated DNA is then added in variable concentration and binds to the streptavidin (C). These tagged DNA molecules can then be tracked by TIRFM.

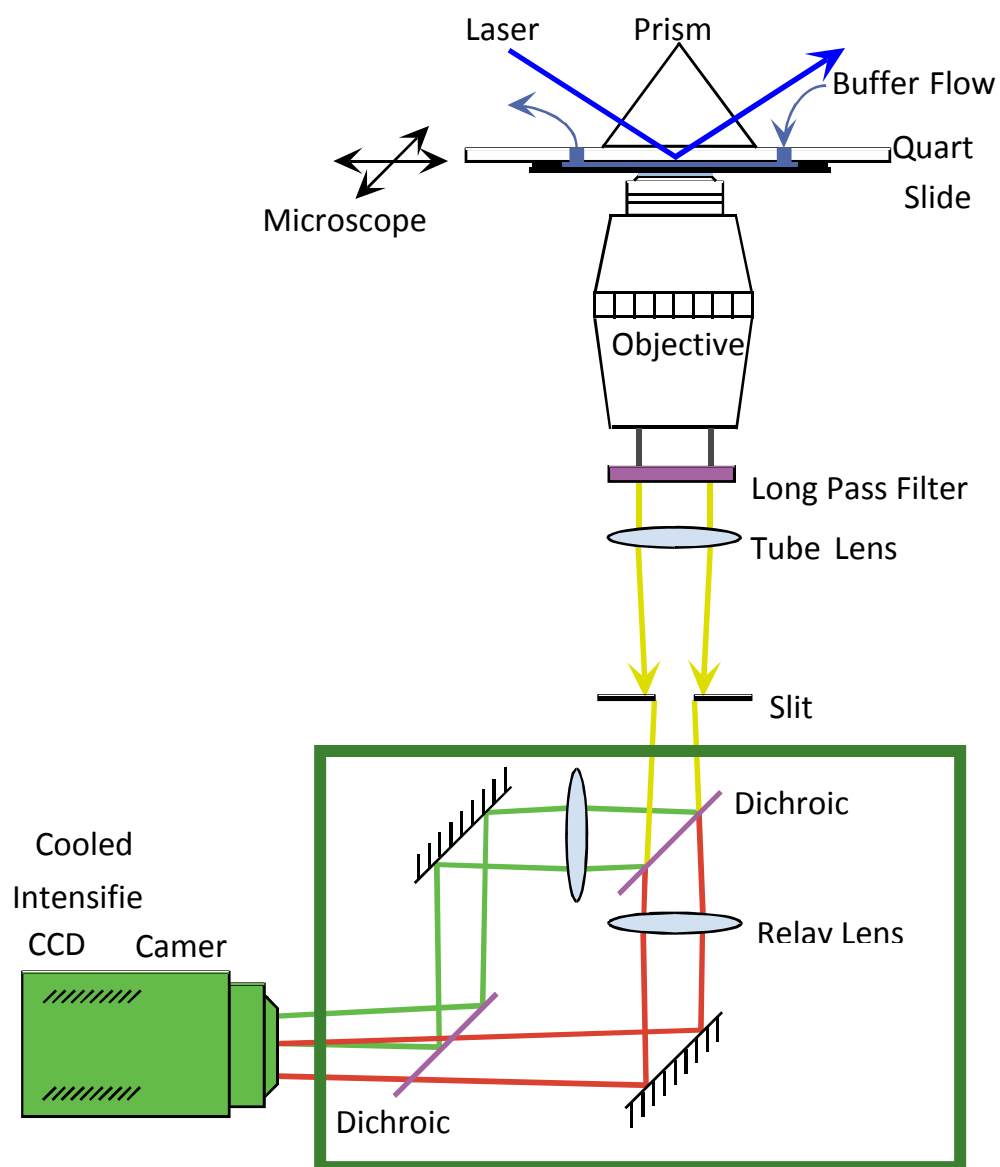


**Figure 6:** Setup of TIR microscope used with the ability to detect both a donor and acceptor fluorophore. For the purposes of TIRF of SLBs only the donor frequency (green) was utilized.

Courtesy of Ivan Rasnik.

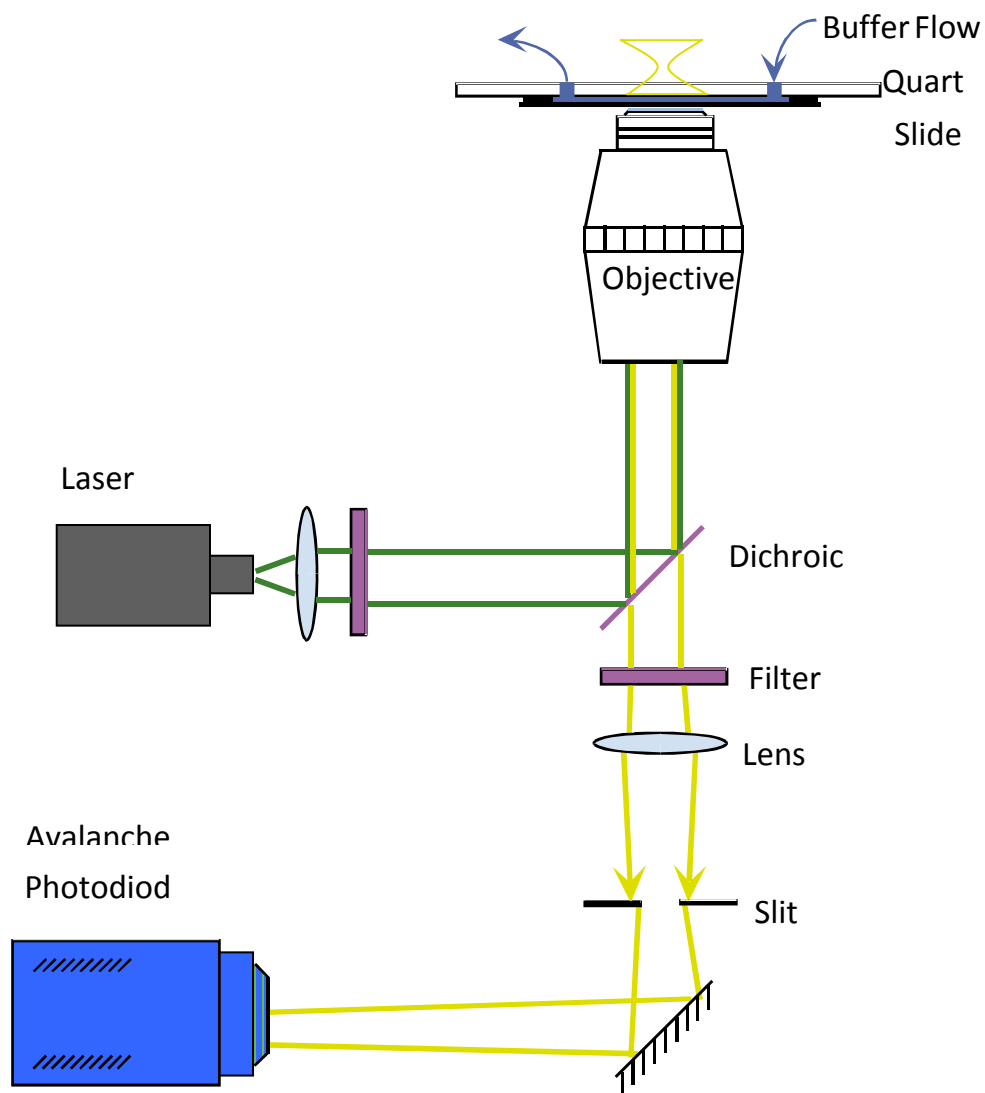


**Figure 7:** Setup of the single photon FCS microscope utilized. Data from the Avalanche Photodiode (APD) was analyzed directly by Labview software.

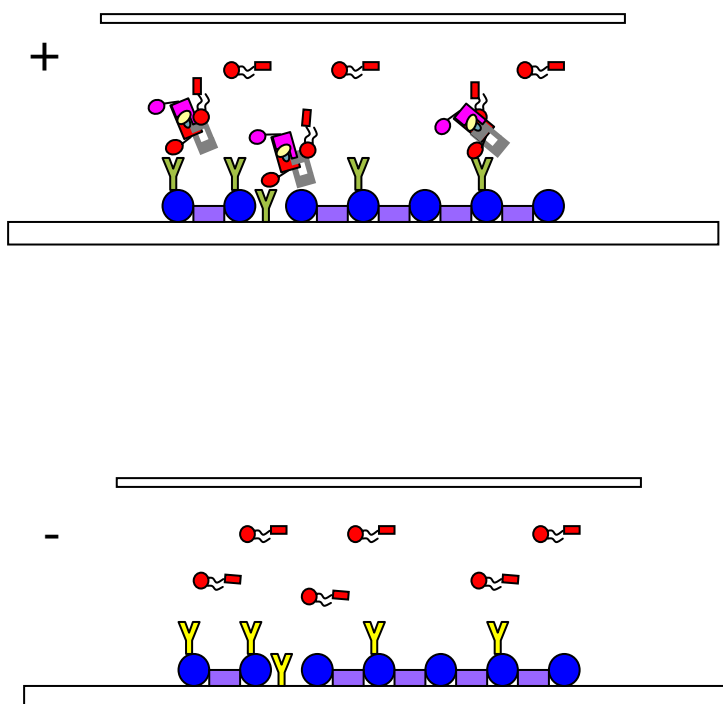


**Figure 8:** Diagram of AP-3 bound to AP-3 binding antibody SA4 delta bound to the quartz slide by protein G (+). The Control situation (-) with the LAMP1 non-cytosolic protein bound is also shown. Both are shown with labeled PI4P in solution, theoretically bound in the (+) scenario and unbound in the (-).

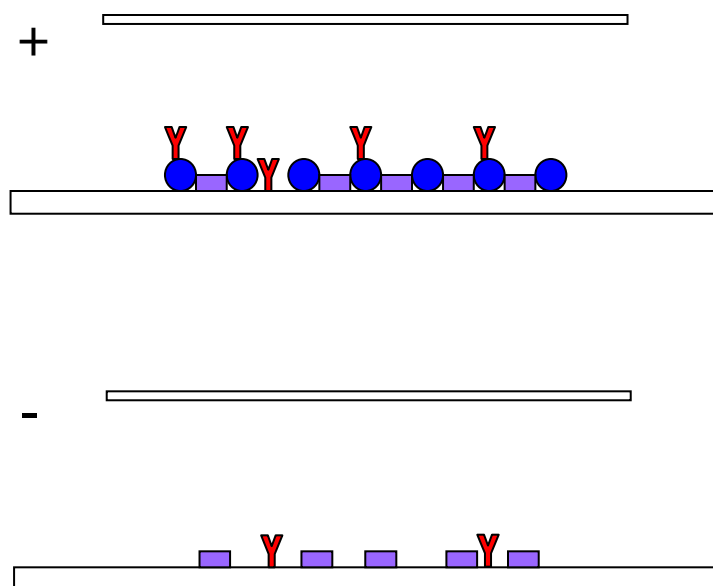


**Figure 9:** Diagram of experiment checking for nonspecific binding for the AP-3 immobilization experiment. A Texas Red labeled antibody should binds with high affinity to Protein G bound to the quartz slide (+) and with little affinity when nonspecifically bound to the slide only (-).

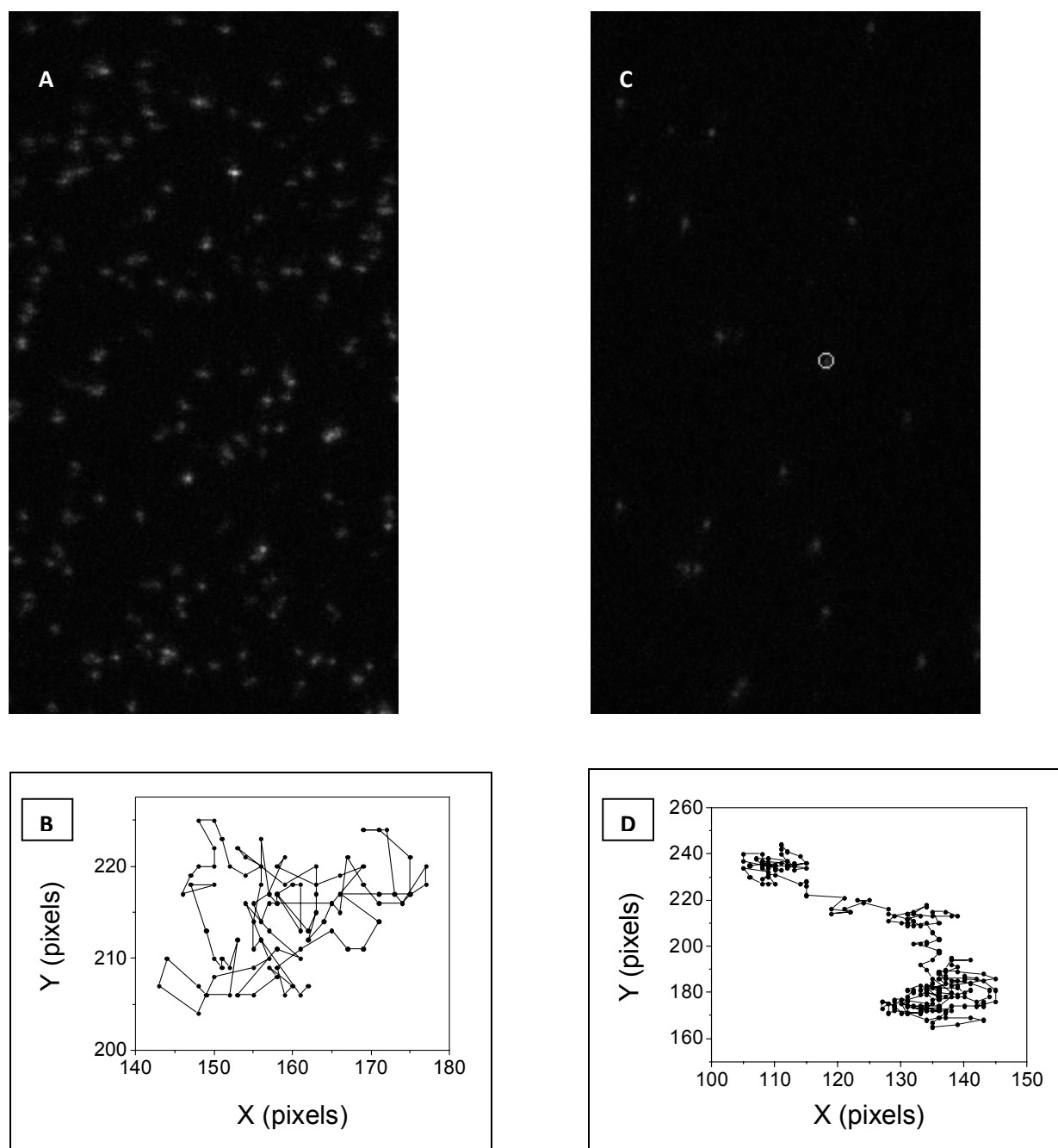


**Figure 10:** TIR image of Rhodamine PE labeled bilayer (A) and trace of RhPE labeled molecular trajectories (B) compared to TIR image of Biotin labeled bilayer (C) and trace of Biotin labeled molecular trajectories (D).

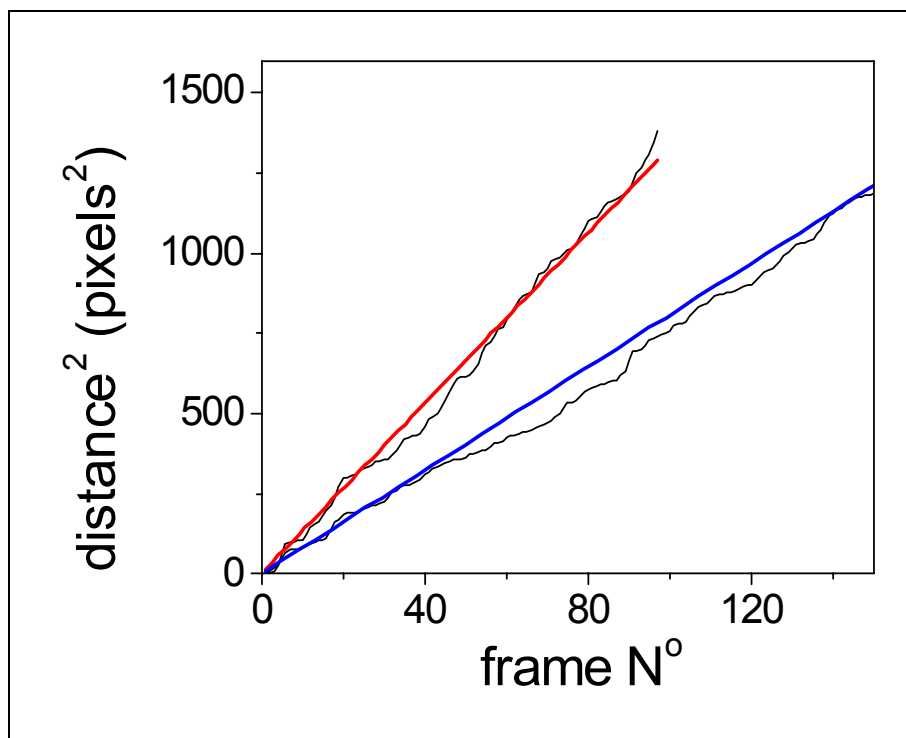


**Figure 11:** Graph of distance of a labeled lipids (in pixels<sup>2</sup>) vs Time (in frames). The area traveled for the RhPE lipids per frame is much higher than the distance traveled for the streptavidin bound biotinylated lipids (blue). The slope of the graphs are the diffusion coefficients for the respective samples in pixels<sup>2</sup> per frame.

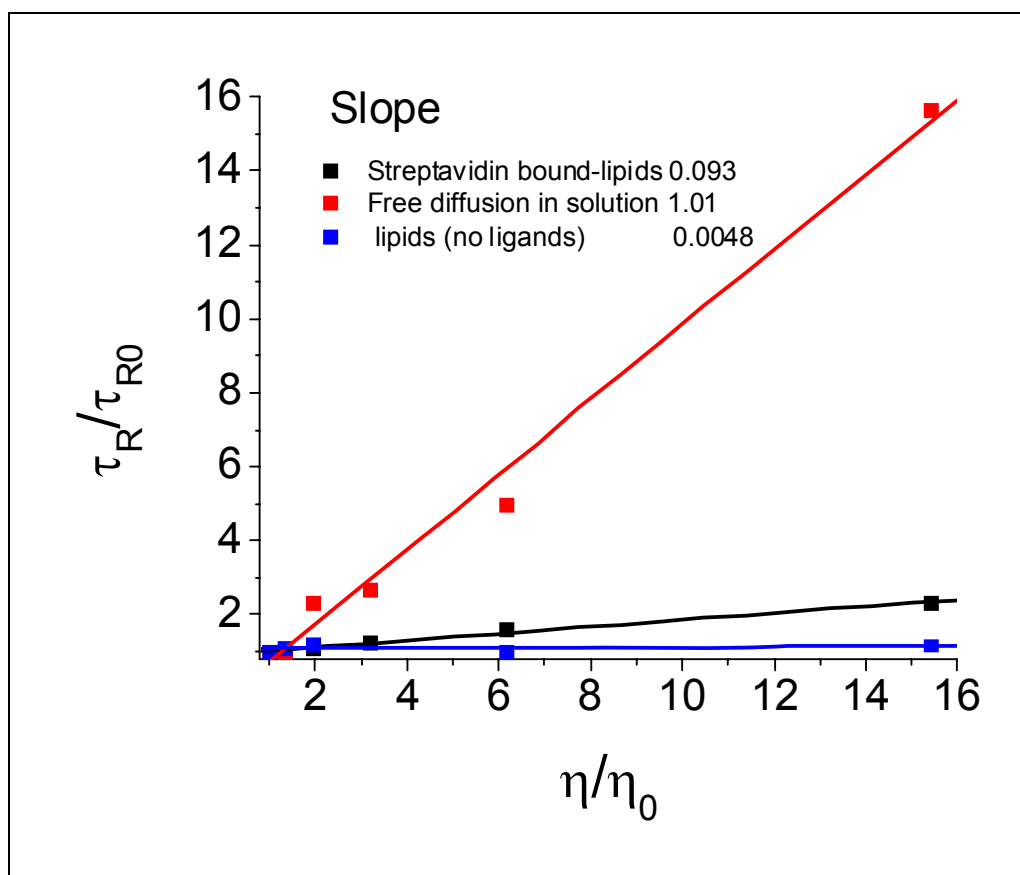


**Figure 12:** Graph of corrected residence time  $\tau_R/\tau_{R0}$  versus viscosity (based on sucrose concentration) for streptavidin bound lipids (black), free diffusion of Rhodamine dye in solution (red) and RhPE labeled lipids in a SLB (blue).  $\tau_R$  is corrected to the residence time of all three samples at 0% sucrose ( $\tau_{R0}$ ) for purposes of comparison. The slope corresponds inversely with the diffusion coefficient of the labeled species. An increase in the slope for the streptavidin bound-lipids illustrates a decrease in diffusion as an effect of increased buffer viscosity while RhPE labeled bilayers show no change. Rhodamine 6G in solution has a linear relationship in diffusion with viscosity.

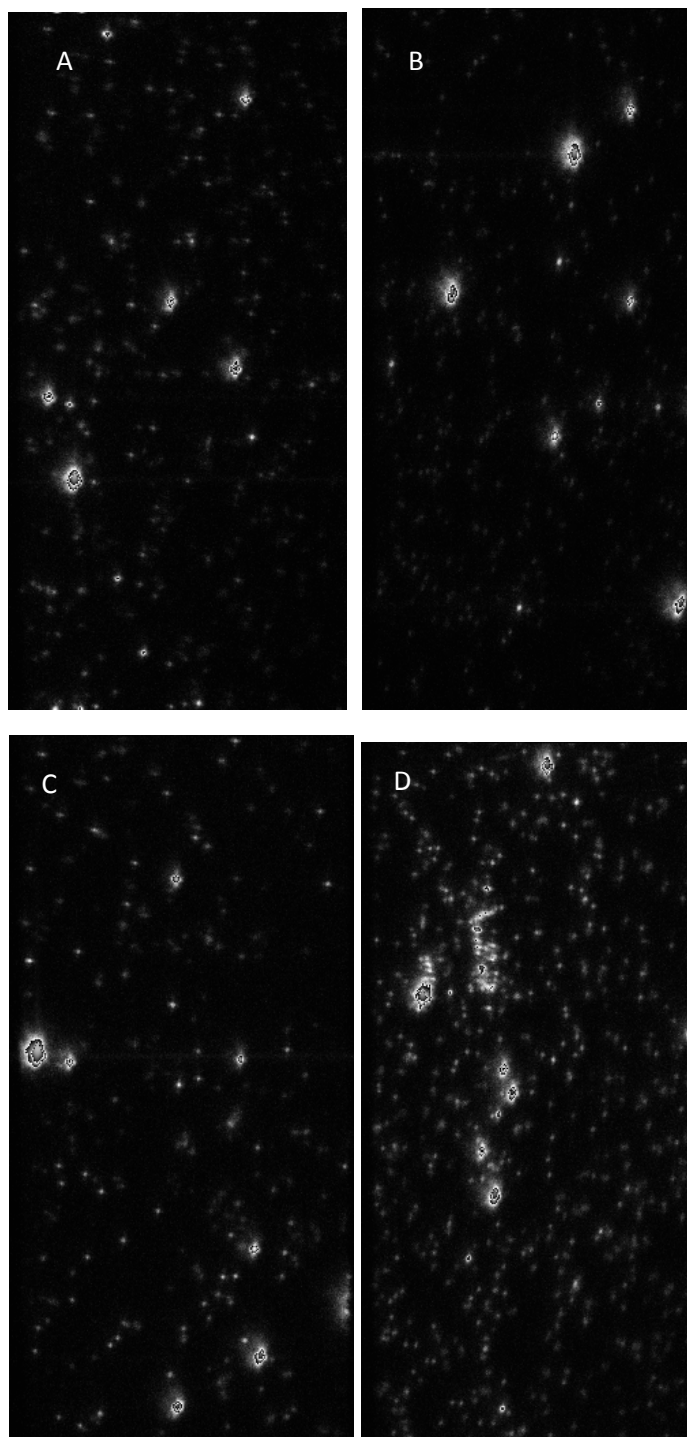


**Figure 13:** Images of SLBS by TIRFM showing (A) a PI4P containing bilayer; (B) a PI(4,5)P2 containing bilayer, (C) a PI4P containing bilayer in the presence of AP-3; (D) a PI(4,5)P2 containing bilayer in the presence of AP-3. Aggregates and immobile fractions visible in all samples obstructed the use of SPT on these systems.

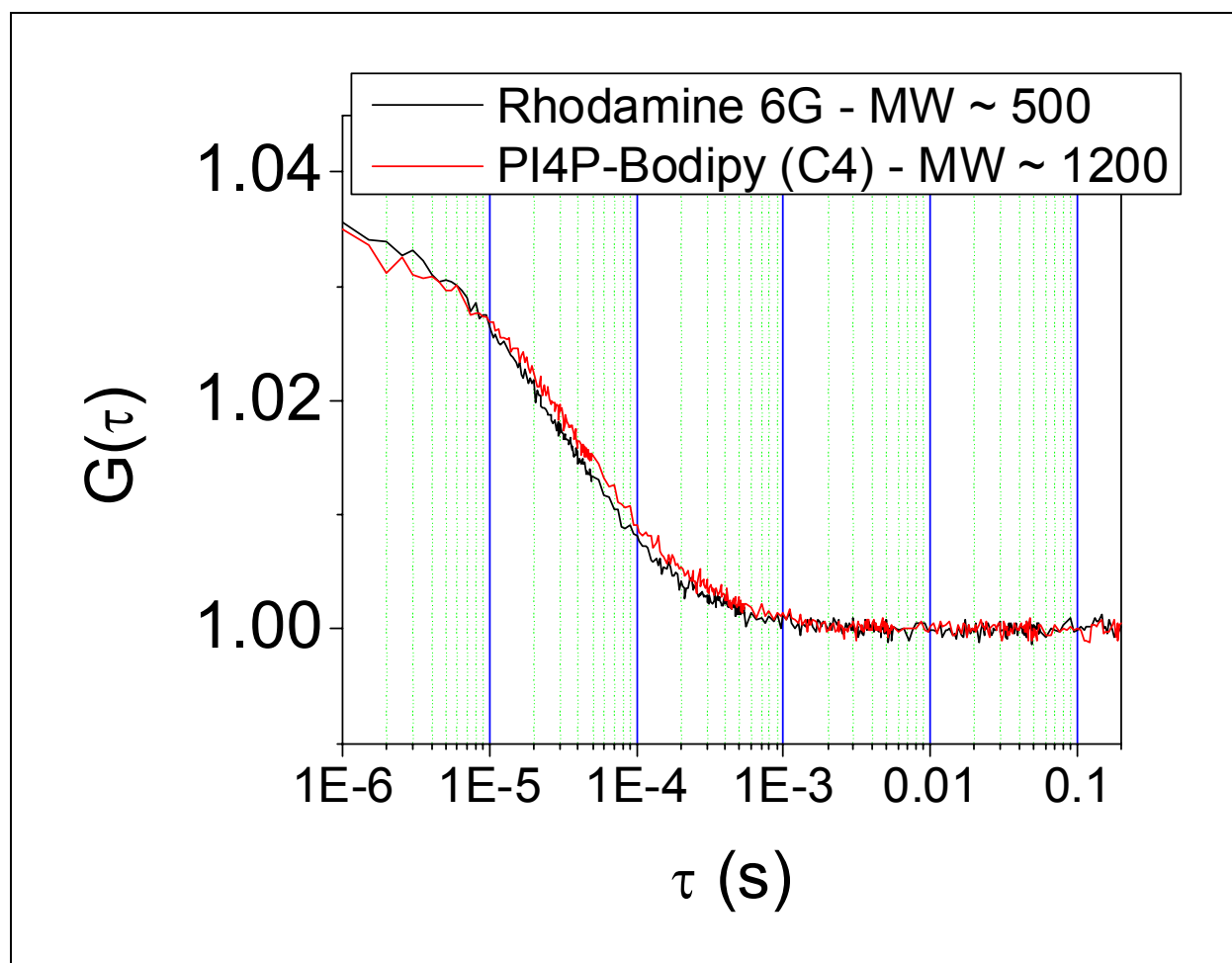


**Figure 14:** Average fluorescence curves from FCS of Rhodamine 6G in solution and BODIPY labeled PI4P. The diffusion coefficient of Rhodamine 6G is 30% greater than the BODIPY labeled PI4P when calculated from the slopes of the curves after fitted with an autocorrelation function.

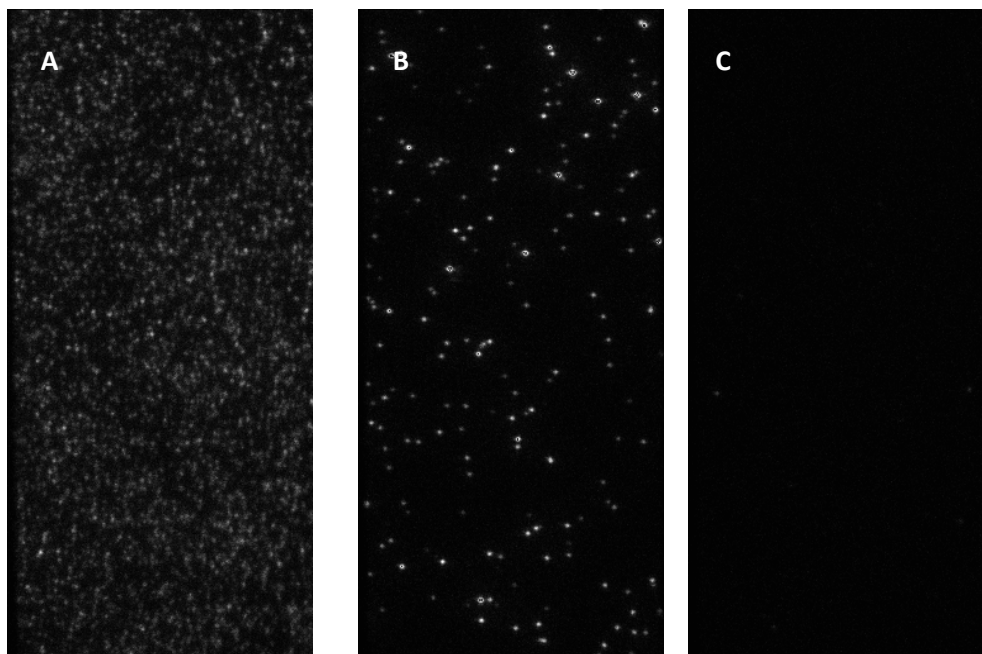


**Figure 15:** TIR Images of Protein G bound Quartz slide with labeled antibody (A), slide with labeled antibody and no Protein G (B), and slide without any labeled antibody (C). All slides contain BSA.

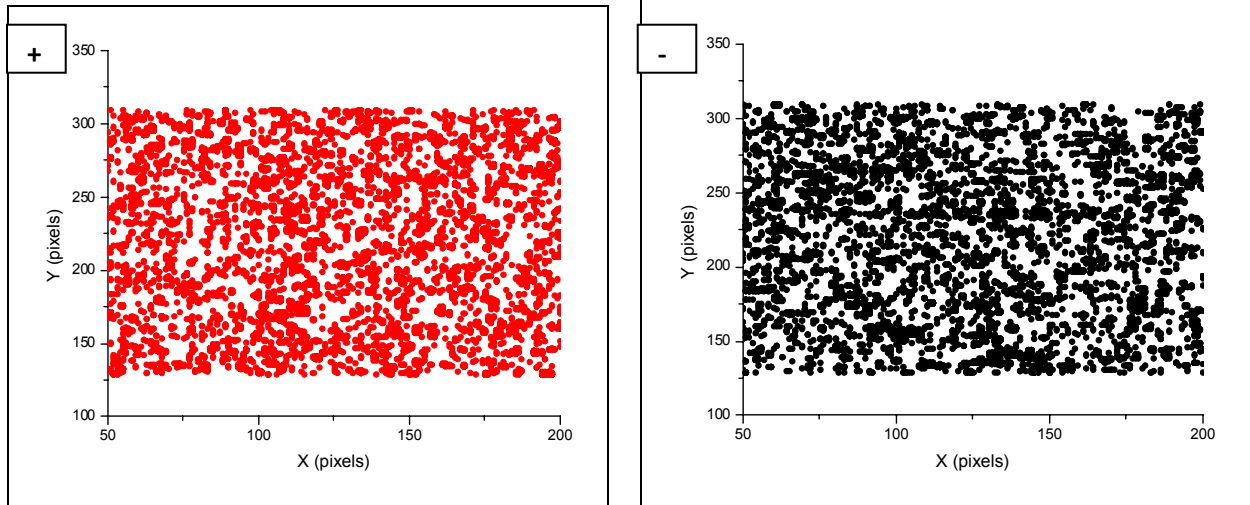


**Figure 16:** Graph showing number of Fluorescently tagged PI4P in slide with AP-3 binding antibody anti-delta SA4 (+) and non-cytosolic LAMP1 binding antibody (-)

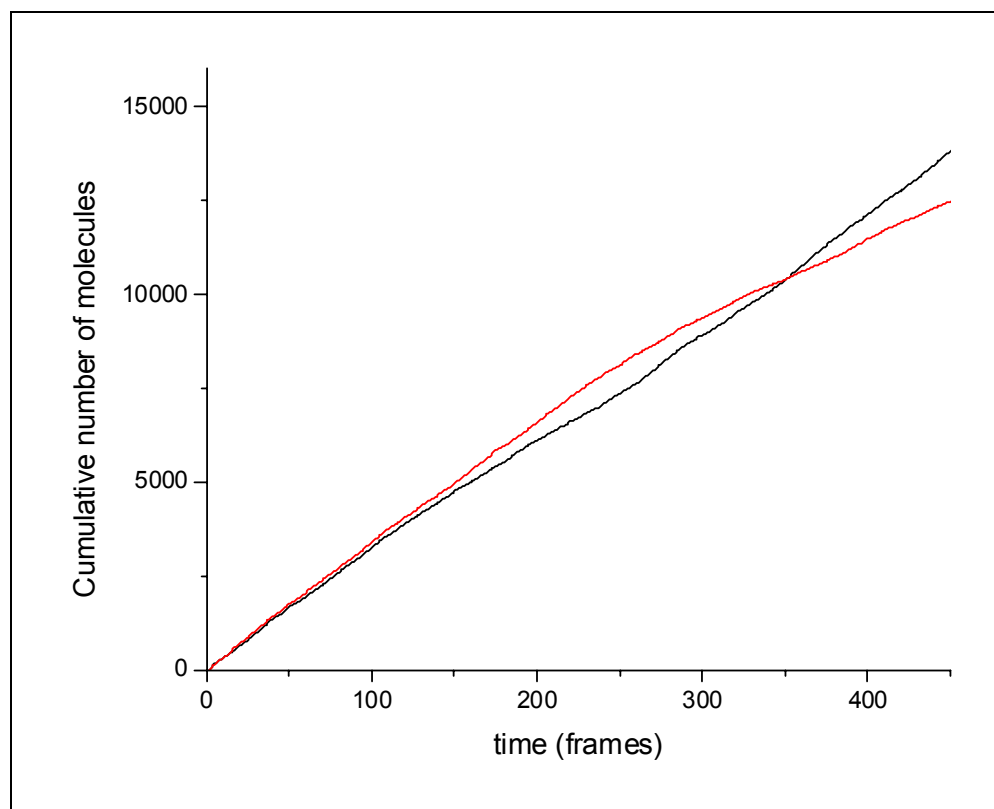


**Figure 17:** Graph of Cumulative number of PI4P molecules vs. Time (in frames) showing slides with AP-3 binding antibody SA4 delta (red) and non-cytosolic LAMP1 binding antibody (black).

**Table 1- sucrose solutions, composition, viscosity, density  
at 20°C**

<b>% Sucrose</b>	<b>gm/L</b>	<b><math>\eta / \eta_w</math></b>	<b><math>\rho</math></b>
0	0	1.00	0.998
5	50.9	1.144	1.018
10	103.8	1.333	1.038
15	158.90	1.589	1.059
20	216.20	1.941	1.081
25	275.90	2.442	1.104
30	338.10	3.181	1.127
35	402.90	4.314	1.151
40	470.60	6.150	1.176
45	541.10	9.360	1.203
50	614.80	15.400	1.230
55	691.60	28.02	1.258
60	771.90	58.37	1.286
65	855.60	146.90	1.316
70	943.00	480.60	1.347
75	1034.00	2323.00	1.379

Table showing viscosities of aqueous solutions ( $\eta / \eta_w$ ) at various concentrations of sucrose (Hofmann, 1977).

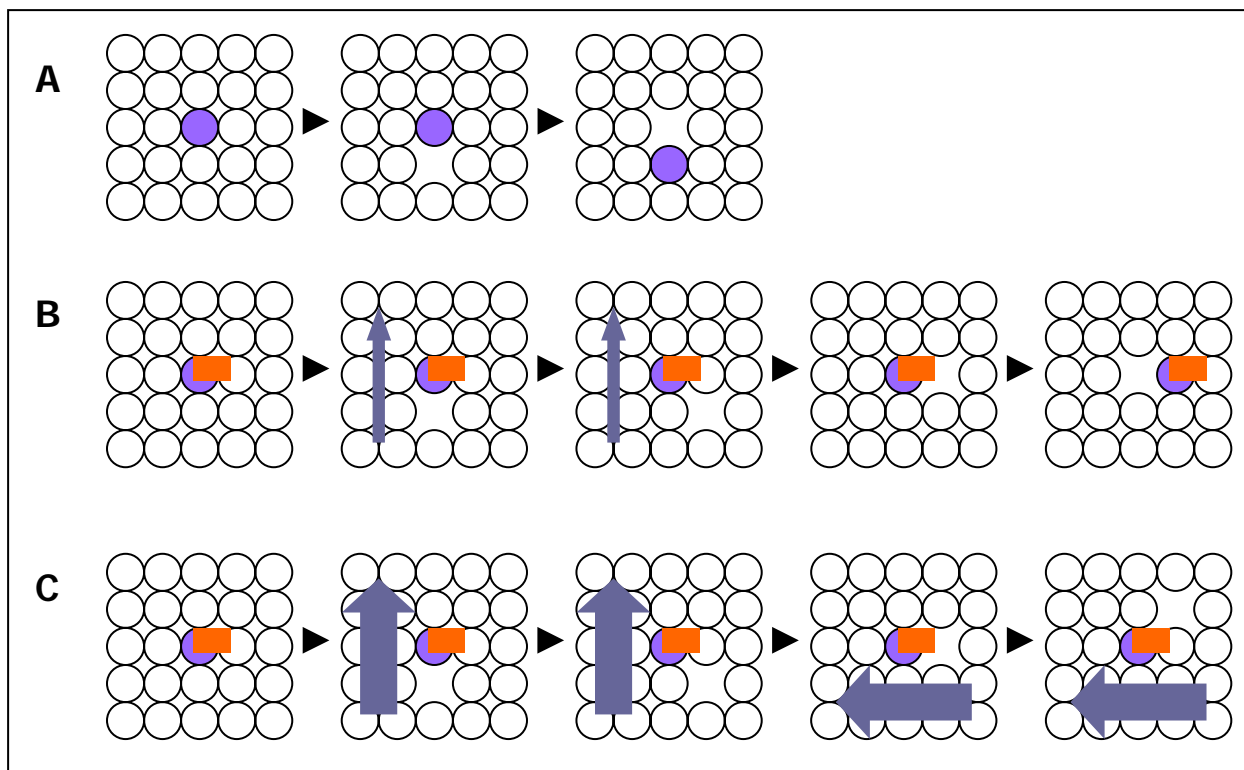


**Figure 18:** Diagram of bilayers illustrating (A) an individual lipid diffusing into an open space adjacent to it within the bilayer compared to (B) a protein (streptavidin) bound lipid missing the opportunity to diffuse into the open space because of the drag added by the bound protein. It has to wait for another somehow more favorable opportunity to diffuse. Drawing (C) shows increased difficulty for protein bound lipid diffusion with greater viscosity in the environment.